Article

Practical Route to Relative Diffusion Coefficients and Electronic Relaxation Rates of Paramagnetic Metal Complexes in Solution by Model-Independent Outer-Sphere NMRD. Potentiality for MRI Contrast Agents

Pascal H. Fries, Christelle Gateau, and Marinella Mazzanti

J. Am. Chem. Soc., **2005**, 127 (45), 15801-15814• DOI: 10.1021/ja052800l • Publication Date (Web): 21 October 2005

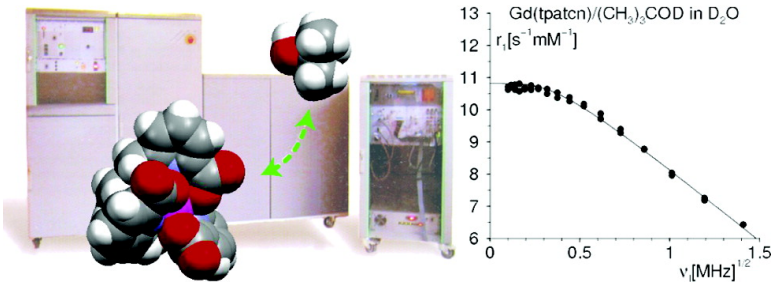

More About This Article

Additional resources and features associated with this article are available within the HTML version:

- Supporting Information
- Links to the 7 articles that cite this article, as of the time of this article download
- Access to high resolution figures
- Links to articles and content related to this article
- Copyright permission to reproduce figures and/or text from this article

View the Full Text HTML

J|A|C|S
ARTICLES
Published on Web 10/21/2005

Practical Route to Relative Diffusion Coefficients and Electronic Relaxation Rates of Paramagnetic Metal Complexes in Solution by Model-Independent Outer-Sphere NMRD. Potentiality for MRI Contrast Agents

Pascal H. Fries,* Christelle Gateau, and Marinella Mazzanti

Contribution from the Laboratoire de Reconnaissance Ionique, Service de Chimie Inorganique et Biologique (UMR-E 3 CEA-UJF), CEA/DSM/Département de Recherche Fondamentale sur la Matière Condensée, CEA-Grenoble, F-38054 Grenoble Cédex 9, France

Received April 29, 2005; E-mail: fries@drfmc.ceng.cea.fr

Abstract: The relaxation of electronic spins S of paramagnetic species is studied by the field-dependence of the longitudinal, transverse, and longitudinal in the rotating frame relaxation rates R_1, R_2, and $R_{1\rho}$ of nuclear spins I carried by dissolved probe solutes. The method rests on the model-independent low-frequency dispersions of the outer-sphere (OS) paramagnetic relaxation enhancement (PRE) of these rates due to the three-dimensional relative diffusion of the complex with respect to the probe solute. We propose simple analytical formulas to calculate these enhancements in terms of the relative diffusion coefficient D, the longitudinal electronic relaxation time T_{1e}, and the time integral of the time correlation function of the $I-S$ dipolar magnetic interaction. In the domain of vanishing magnetic field, these parameters can be derived from the low-frequency dispersion of R_1 thanks to sensitivity improvements of fast field-cycling nuclear relaxometers. At medium field, we present various approaches to obtain these parameters by combining the rates R_1, R_2, and $R_{1\rho}$. The method is illustrated by a careful study of the proton PREs of deuterated water HOD, methanol CH_3OD, and *tert*-butyl alcohol $(CH_3)_3COD$ in heavy water in the presence of a recently reported nonacoordinate Gd(III) complex. The exceptionnally slow electronic relaxation of the Gd(III) spin in this complex is confirmed and used to test the accuracy of the method through the self-consistency of the low- and medium-field results. The study of molecular diffusion at a few nanometer scale and of the electronic spin relaxation of other complexed metal ions is discussed.

1. Introduction

Paramagnetic metal ions coordinated by organic ligands play central roles in the preparation of molecular nanomagnets,[1−2] the structure and activity of many metal-containing proteins,[3−4] and the enhancement of image contrast in magnetic resonance imaging[5,6] (MRI). Besides the applied use, the paramagnetism of a metal ion is a unique tool to explore the structure and dynamics of its environment and hence to optimize the underlying molecular factors in view of the applications: First, the equilibrium magnetic properties of the metal and the time correlation functions (TCF) of its magnetic moment are direct probes of its electronic interactions with the neighboring atoms. Second, the paramagnetic effects induced on the nuclear spins give invaluable information, intrisically very long range, about their positions with respect to the metal.

Among the observables due to a paramagnetic center, NMR paramagnetic relaxation enhancement (PRE) is a versatile spectroscopic property, which gives access to dynamical processes happening over a time scale ranging from about 10^{-12} to 10^{-6} s. It allows one to explore the magnetic energy levels of the ion and hence its electronic interactions with the ligands. It gives information about the spatial equilibrium distribution of the nuclear spins located both on the complex and on surrounding species. It probes a wide variety of intramolecular processes including the time distortion of the complex, its Brownian rotation, and the resulting electronic relaxation of the magnetic moment of the ion. It can be used to study the dynamics of molecular recognition of the complexed ion by the solvent and solutes.

Complexes of paramagnetic metal ions are used in MRI to accelerate the relaxation of the water proton nuclear spins I in the surrounding tissue[5,6] thanks to the strong magnetic dipole−dipole interaction of these nuclear spins with the electronic spins S of the metal ions. This local increase of nuclear relaxation rate provides the image contrast. The efficiency of a contrast agent (CA) in terms of image contrast is measured by its relaxivity, i.e. the relaxation rate increase of the nuclear spins per millimole of complexed metal ions. Today, even though

(1) Sangregorio, S.; Ohm, T.; Paulsen, C.; Sessoli, R.; Gatteschi, D. *Phys. Rev. Lett.* **1997**, *78*, 4645−4648.
(2) Kahn, O. *Molecular Magnetism*; VCH: New York, 1993.
(3) Bertini, I.; Luchinat, C.; Parigi, G. *Solution NMR of Paramagnetic Molecules*; Elsevier: Amsterdam, 2001.
(4) *Handbook of Metalloproteins*; Messerschmidt, A., Huber, R., Wieghardt, K., Poulos, T., Eds.; John Wiley: New York, 2001.
(5) Caravan, P.; Ellison, J. J.; McMurry, T. J.; Lauffer, R. B. *Chem. Rev.* **1999**, *99*, 2293−2352.
(6) *The Chemistry of Contrast Agents in Medical Magnetic Resonance Imaging*; Merbach, A. E., Tóth, É., Eds.; John Wiley: New York, 2001.

10.1021/ja052800l CCC: $30.25

Mn(II) complexes look promising for specialized applications,[7,8] Gd(III) chelates are by far the most widely used contrast agents in clinical practice. Indeed, Gd(III) presents the highest magnetic moment ($S = {}^7/_2$) of any element and a slow electronic relaxation that make it ideal as a relaxation agent. However the relaxivity of currently used CAs is only a few percent of the maximal theoretical relaxivity. The "new generation" target specific contrast agents require higher relaxivity. The simultaneous optimization of the molecular parameters determining the relaxivity (electronic relaxation, water-exchange, rotation dynamics of the whole complex, solvation, ion-nuclear distance) is essential to prepare more efficient contrast agents.

Considerable experimental and theoretical efforts have been spent over the last 20 years[5−14] in order to discover and optimize the molecular factors affecting the relaxivity. Unfortunately, the experimental characterization of the Gd(III) electronic relaxation[3,5,6] and its rigorous theoretical description are still open issues[7,15] despite numerous attempts. Powell et al.[16] pioneered the thorough investigation of Gd(III) transverse electronic relaxation by multifrequency and multitemperature EPR experiments. To interpret these extensive data, the Grenoble and Lausanne groups[17−19] had to reconsider the molecular mechanisms at the origin of the electronic relaxation. They introduced the modulation of the static, i.e., vibration-averaged, zero-field splitting (ZFS) by the rotational diffusion of the complex and showed how its relative contribution to the EPR spectra varies with resonance frequency and temperature.[18] The presence of a static ZFS leads to the additional difficulty that the electronic relaxation at low field can often no longer be described by the second-order time-dependent perturbation approximation of Redfield. Therefore, Monte Carlo simulations beyond the Redfield limit were proposed to compute the quantum TCFs of the electronic spin.[20,21] These theoretical improvements together with relaxation formalisms adapted to slowly rotating complexes[22,23] provide a framework intended to explain the nuclear and electronic relaxation of several CAs, both of standard and high molecular weights, in terms of structural and dynamic molecular properties.

The major obstacle to getting a clear understanding of the effects of the longitudinal electronic relaxation time T_{1e} on the relaxivity at the magnetic field values 0.5 to 11 T of the MR imagers is that T_{1e} is too short for an easy direct measurement.[24,25] Here we describe an indirect, but model-independent, PRE method for measuring the longitudinal electronic relaxation rate $1/T_{1e}$ of a Gd(III)-based CA both at zero-field and above 0.5 T. The method rests on molecular probes carrying the observed relaxing nuclear spins and undergoing relative translational Brownian motions with respect to the CA. It also provides the relative diffusion coefficients $D = D_{probe} + D_{CA}$ of the CA with respect to the probes. Diffusion coefficients are useful to estimate molecular radii and are key parameters of the outer-sphere contribution to the CA relaxivity,[5,6] besides their importance in transport properties.[26] The self-consistency and accuracy of the method will be demonstrated through a careful multifield PRE study of the protons on various probes displaying different sizes and self-diffusion coefficients, in heavy water D_2O in the presence of the recently reported nonacoordinate Gd(tpatcn) complex[27] (tpatcn = (1,4,7-tris[(6-carboxypyridin-2-yl)methyl]-1,4,7-triazacyclononane). This complex is particularly suitable for validating our method due to its low-field electronic relaxation time which was predicted to have an exceptionally long value[27] $10^{-9}-10^{-8}$ s. Previous crystallographic studies have shown that the tripodal ligand tpatcnH_3 formed by addition of three pyridinecarboxylate arms to the macrocyclic core 1,4,7-triazacyclonane is well adapted to the coordination of lanthanides ions of different sizes and leads to complexes which do not have water molecules coordinated to the metal center. Proton NMR spectroscopic studies indicated that the C3-symmetric solid-state structure is retained in solution where the macrocyclic framework remains bound and rigid on the NMR spectroscopic time scale. Since the Gd(tpatcn) complex has no water molecule directly bound to the metal ion, it was suggested that an especially slow electronic spin relaxation might be the origin of the observed high relaxivity of the water protons at low field.

The PREs were measured between 10 kHz and 500 MHz. Low-frequency longitudinal relaxation studies of semidilute nuclei with short relaxation times have been made possible by the recent sensitivity enhancement of fast field cycling (FFC) relaxometers.[28,29] The molecules of water HOD, methanol CH_3-OD, and *tert*-butyl alcohol $(CH_3)_3$COD were chosen as probes because of their quite different sizes and self-diffusion coefficients.

The paper is organized as follows: In section 2, the outer-sphere (OS) PRE theory at the basis of our determination of the relative diffusion coefficients D and electronic relaxation rates $1/T_{1e}$ is recalled. The general expressions of the OS longitudinal, transverse, and longitudinal in the rotating frame PREs are given in terms of the time correlation function (TCF)

(7) Troughton, J. S.; Greenfield, M. T.; Greenwood, J. M.; Dumas, S.; Wiethoff, A. J.; Wang, J.; Spiller, M.; McMurry, T. J.; Caravan, P. *Inorg. Chem.* **2004**, *43*, 6313−6323.
(8) Nordhøy, W.; Anthonsen, H. W.; Bruvold, M.; Brurok, H.; Skarra, S.; Krane, J.; Jynge, P. *Magn. Reson. Med.* **2004**, *52*, 506−514.
(9) Botta, M. *Eur. J. Inorg. Chem.* **2000**, 399−407.
(10) Aime, S.; Botta, M.; Fedeli, F.; Gianolio, E.; Terreno, E.; Anelli, P. *Chem. Eur. J.* **2001**, *7*, 5262−5269.
(11) Li, W.; Parigi, G.; Fragai, M.; Luchinat, C.; Meade, T. J. *Inorg. Chem.* **2002**, *41*, 4018−4024.
(12) Vander Elst, L.; Port, M.; Raynal, I.; Simonot, C.; Muller, R. N. *Eur. J. Inorg. Chem.* **2003**, 2495−2501.
(13) Thompson, M. K.; Botta, M.; Nicolle, G.; Helm, L.; Aime, S.; Merbach, A. E.; Raymond, K. M. *J. Am. Chem. Soc.* **2003**, *125*, 14274−14275.
(14) Pierre, V. C.; Botta, M.; Raymond, K. N. *J. Am. Chem. Soc.* **2005**, 127, 504−505.
(15) Zhou, X.; Caravan, P.; Clarkson, R. B.; Westlund, P. O. *J. Magn. Reson.* **2004**, *167*, 147−160.
(16) Powell, D. H.; Dhubhghaill O. M. N.; Pubanz, D.; Helm, L.; Lebedev, Y. S.; Schlaepfer, W.; Merbach, A. E. *J. Am. Chem. Soc.* **1996**, *118*, 9333−9346.
(17) Rast, S.; Fries, P. H.; Belorizky, E. *J. Chim. Phys.* **1999**, *96*, 1543−1550.
(18) Rast, S.; Fries, P. H.; Belorizky, E. *J. Chem. Phys.* **2000**, *113*, 8724−8735.
(19) Rast, S.; Borel, A.; Helm, L.; Belorizky, E.; Fries, P. H.; Merbach, A. E. *J. Am. Chem. Soc.* **2001**, *123*, 2637−2644.
(20) Schaefle, N.; Sharp, R. *J. Chem. Phys.* **2004**, *121*, 5387−5394.
(21) Rast, S.; Fries, P. H.; Belorizky, E.; Borel, A.; Helm, L.; Merbach, A. E. *J. Chem. Phys.* **2001**, *115*, 7554−7563.
(22) Bertini, I.; Galas, O.; Luchinat, C.; Parigi, G. *J. Magn. Reson., Ser. A* **1995**, *113*, 151−158.
(23) Kruk, D.; Nilson, T.; Kowalewski, J. *Phys. Chem. Chem. Phys.* **2001**, *3*, 4907−4917.
(24) Borel, A.; Helm, L.; Merbach, A. E.; Atsarkin, V. A.; Demidov, V. V.; Odintsov, B. M.; Belford, R. L.; Clarkson, R. B. *J. Phys. Chem. A* **2002**, *106*, 6229−6231.
(25) Borel, A.; Yerly, F.; Helm, L.; Merbach, A. E. *J. Am. Chem. Soc.* **2002**, *124*, 2042−2048.
(26) Callaghan, P. T. *Principles of Nuclear Magnetic Resonance Microscopy*; Clarendon Press: Oxford, 1995.
(27) Gateau, C.; Mazzanti, M.; Pécaut, J.; Dunand, F. A.; Helm, L. *J. Chem. Soc., Dalton Trans.* **2003**, 2428−2433.
(28) Anoardo, E.; Galli, G.; Ferrante, G. *Appl. Magn. Reson.* **2001**, *20*, 365−404.
(29) Fries, P. H.; Ferrante, G.; Belorizky, E.; Rast, S. *J. Chem. Phys.* **2003**, *119*, 8636−8644.

$g_2(t)$ of the dipolar magnetic interaction of the observed nuclear spin I with the Gd(III) electronic spin S. Low- and medium-field ranges are defined with respect to the values of D and $1/T_{1e}$. In both ranges, when the molecular probe carrying the nuclear spin I has no charge−charge Coulomb interaction with the Gd(III) complex, simple low-frequency expressions of the PREs in terms of D and $1/T_{1e}$ are derived from the universal long-time $t^{-3/2}$ behavior of $g_2(t)$ resulting from the three-dimensional character of the relative translational Brownian motion of the two species.[30−37] Section 3 deals with the experimental details relative to the preparation of the paramagnetic solutions used to assess our method and to the PRE measurements. The experimental data are interpreted in section 4, where the relative diffusion coefficients D for the various probes together with the values of $1/T_{1e}$ are obtained. The self-consistency and accuracy of the method are discussed with particular emphasis on the additional cross-checking provided by the slow electronic relaxation of Gd(tpatcn) at low field, which allows one to derive the values of D and of the dipolar TCF integral $\int_0^\infty g_2(t)\,dt$ at low field and to compare them with those obtained in the medium-field range. Section 5 is a guide to the practical implementation of the method. In the last section, the extension of the method to various paramagnetic centers in solution and its potentiality to give insight into additional microdynamic features are reviewed.

2. Theory

2.1. Outer-Sphere Paramagnetic Relaxation Enhancement. In a liquid solution placed in an external magnetic field $\mathbf{B}_0$, we consider dilute Gd(III) complexes GdL moving with respect to solvent or solute molecules M_I carrying nuclear spins I. The longitudinal relaxation rate R_1, transverse relaxation rate R_2, or longitudinal relaxation rate $R_{1\rho}$ in the rotating frame[38] of the nuclear spins I in this paramagnetic (p) solution is the sum[5,6]

$$R_\alpha = R_{\alpha 0} + R_{\alpha p}\ (\alpha = 1, 2, 1\rho) \tag{1}$$

of the value $R_{\alpha 0}$ in the diamagnetic solution without GdL complexes and of the paramagnetic relaxation enhancement (PRE) $R_{\alpha p}$ of the nuclear spins I due to their interactions with the electronic spins S of the complexed Gd(III) ions. The PRE $R_{\alpha p}$ is conveniently[10] described as the sum

$$R_{\alpha p} = R_{\alpha p}^{IS} + R_{\alpha p}^{2S} + R_{\alpha p}^{OS} \tag{2}$$

of the inner-sphere (IS), second-sphere (2S), and outer-sphere (OS) contributions $R_{\alpha p}^{IS}$, $R_{\alpha p}^{2S}$, and $R_{\alpha p}^{OS}$, corresponding, respectively, to random intermolecular trajectories where, at initial time $t = 0$, M_I directly coordinates Gd(III), has a noncovalent binding association to the ligand L, and undergoes a relative translational diffusion with respect to GdL. We will focus on the OS relaxation contributions $R_{\alpha p}^{OS}$, since they provide us with the main and measurable sources of PRE dispersion at low resonance frequency. The OSPREs $R_{\alpha p}^{OS}$ are assumed to stem[5,6,29] from the random fluctuations of the dipolar magnetic interactions H_{IS}^{dip} of I with the Gd(III) electronic spins S of the various GdL complexes. More precisely, they are due to the fluctuations of H_{IS}^{dip} created by (i) the relative translational diffusion of GdL with respect to M_I modulated by the Brownian rotational motions of the two species and (ii) the quantum dynamics of the electronic spins S.

Denote the vector joining the nuclear spin I of a molecule M_I to the electronic spin S of a GdL complex by $\mathbf{r}$. Let (r,θ,ϕ) be its spherical coordinates in the laboratory (L) frame, the z axis of which is taken to be parallel to $\mathbf{B}_0$. The key quantity of the intermolecular PRE is the dipolar time correlation function (TCF) $g_2(t)$ of the random functions $r^{-3}Y_{2q}(\theta,\phi)$ of the interspin vector $\mathbf{r}$. It is defined as[31−34]

$$g_2(t) \equiv \langle r_{t=0}^{-3} Y_{2q}(\theta_{t=0},\phi_{t=0}) r_t^{-3} Y_{2q}^*(\theta_t,\phi_t)\rangle \tag{3}$$

and accounts for the relaxing contributions from all the GdL complexes, so that it is proportional to their number density N_S

$$g_2(t) = N_S \int\int \frac{Y_{2q}(\theta_0,\phi_0)}{r_0^{\,3}} \frac{Y_{2q}^*(\theta,\phi)}{r^3} g_{IS}^{site-site}(r_0)\rho(\mathbf{r}_0,\mathbf{r},t)\,d\mathbf{r}_0\,d\mathbf{r} \tag{4}$$

where $g_{IS}^{site-site}(r_0)$ is the pair distribution function of the interspin distance, and $\rho(\mathbf{r}_0,\mathbf{r},t)$, the propagator describing the random evolution of the interspin vector $\mathbf{r}$ in the course of time. Because of the rotational invariance of $g_{IS}^{site-site}(r_0)$ and $\rho(\mathbf{r}_0,\mathbf{r},t)$, the expression 4 of $g_2(t)$ is independent of the index $q = -2,..., +2$ of the spherical harmonics Y_{2q}. Considerable efforts have been spent to calculate $g_2(t)$, or equivalently its Laplace transform

$$\tilde{g}_2(\sigma) \equiv \int_0^\infty g_2(t)\exp(-\sigma t)\,dt \tag{5}$$

and its Fourier−Laplace transform

$$j_2(\sigma) \equiv \frac{1}{\pi}\mathrm{Re}\tilde{g}_2(\sigma) \tag{6}$$

also named spectral density. Analytical expressions of $\tilde{g}_2(\sigma)$ were obtained for spherical species carrying centered[31,32] and off-center spins.[33] However, in the general situation of anisotropic molecular interactions, the analytical formalism becomes very intricate, and only cumbersome approximate expressions could be derived in a few limiting cases.[39]

As usual, let γ_I, γ_S be the gyromagnetic ratios of the nuclear and electronic spins I and S. Denote their angular Larmor resonance frequencies by $\omega_I \equiv -\gamma_I B_0$, $\omega_S \equiv -\gamma_S B_0$. Introduce the dipolar coupling constant A defined as

$$A \equiv \frac{2}{5}\gamma_I^{\,2}\gamma_S^{\,2}h^2 S(S+1) \tag{7}$$

The longitudinal PRE R_{1p} is of particular interest in all the relaxation studies as a function of field. Indeed, like R_{2p} and $R_{1\rho p}$, R_{1p} can be measured at medium and high fields. In addition, using fast field cycling (FFC) relaxometers,[3,5,6,28] its experi-

(30) Harmon, J. F.; Muller, B. H. *Phys. Rev.* **1969**, *182*, 400−410.
(31) Ayant, Y.; Belorizky, E.; Alizon, E.; Gallice, J. *J. Phys. (France)* **1975**, *36*, 991−1004.
(32) Hwang, L. P.; Freed, J. H. *J. Chem. Phys.* **1975**, *63*, 4017−4025.
(33) Ayant, Y.; Belorizky, E.; Fries, P.; Rosset, J. *J. Phys. (France)* **1977**, *38*, 325−337.
(34) Fries, P.; Belorizky, E. *J. Phys. (France)* **1978**, *39*, 1263−1282.
(35) Sholl, C. A. *J. Phys. C* **1981**, *14*, 447−464.
(36) Fries, P. H. *Mol. Phys.* **1983**, *48*, 503−526.
(37) Fries, P. H.; Belorizky, E. *J. Chem. Phys.* **1983**, *79*, 1166−1169.
(38) Canet, D.; Boubel, J. C.; Canet-Soulas, E. *La RMN: Concepts, Méthodes et Applications*; Dunod: Paris, 2002; pp 114−124.
(39) Zeidler, M. D. *Mol. Phys.* **1975**, *30*, 1441−1451.

mental study is possible down to very low field values of about 10^{-4} tesla. The longitudinal OSPRE R_{1p}^{OS} is given by[29]

$$R_{1p}^{OS} = A\left[j_{2||}(\omega_I) + \frac{7}{3}j_{2\perp}(0)\right] \quad (8)$$

where the longitudinal and transverse spectral densities $j_{2||}(\omega_I)$ and $j_{2\perp}(0)$ are the real parts of the Fourier−Laplace transforms

$$j_{2dir}(\omega) \equiv \frac{1}{\pi}\mathrm{Re}\int_0^\infty g_2(t)G_{dir}^{nor}(t)\exp(-i\omega t)\,dt\ (dir = ||, \perp) \quad (9)$$

In eq 9, the normalized electronic TCFs

$$G_{dir}^{nor}(t) \equiv \frac{G_{dir}(t)}{G_{dir}(0)}\ (dir = ||, \perp) \quad (10)$$

are derived from the longitudinal and transverse electronic TCFs

$$G_{||}(t) \equiv \frac{1}{2S+1}\mathrm{tr}[\overline{S_z(t)S_z(0)}] \quad (11)$$

and

$$G_{\perp}(t) \equiv \frac{1}{2S+1}\mathrm{tr}[\overline{S_+(t)S_-(0)}] \quad (12)$$

where the traces are taken over the $2S+1$-dimensional spin space and the bars represent the ensemble average over all the possible evolutions of the electronic spin operators $S_z(t)$ and $S_+(t)$. For the sake of simplifying the notations, the explicit dependence of $G_{dir}^{nor}(t)$ and $j_{2dir}(\omega)$ on B_0 is dropped from the arguments of these functions. It should be noted that the electronic TCF $G_\perp(t)$, which is involved in the definition 9 of the transverse spectral density $j_{2\perp}(0)$ and modulates $g_2(t)$, has much more rapid oscillations than the nuclear Larmor frequency factors $\exp(-i\omega_I t)$ and $\exp(i\omega_I t)$. Therefore, the spectral densities $j_{2\perp}(\pm\omega_I)$ occurring in the rigorous expression of R_{1p}^{OS} are nearly indistinguishable from $j_{2\perp}(0)$ and replaced by the latter.

The simultaneous experimental determination of the relative diffusion constant D of GdL with respect to M_I and of the longitudinal electronic relaxation time T_{1e} of the Gd(III) complexed ion is based on the following three properties:

(P1) Denote the M_I−GdL collision diameter by b. Assume there are no charge−charge Coulomb forces between M_I and GdL, so that their molecular pair distribution function g_{IS} has the ideal gas value 1 at not too long M_I−GdL intercenter distance R, i.e.,

$$g_{IS} \cong 1 \text{ for } R \geq \text{a few collision diameters } b \quad (13)$$

Then, the dipolar TCF $g_2(t)$ shows the long-time decay

$$g_2(t) \cong \frac{N_S}{18\sqrt{\pi}}\frac{1}{D^{3/2}t^{3/2}} \text{ as } t \to \infty \quad (14)$$

This universal behavior of $g_2(t)$, or the equivalent $\sqrt{\omega}$ dispersion of its Fourier−Laplace transform $j_2(\sigma = i\omega)$ in the low-frequency domain, was progressively shown in more and more realistic situations of the interacting spins. First, the property was found for models assuming that the molecules are spherical, have a relative translational diffusion in a viscous continuum, and carry centered[30−32] and off-centered spins.[33] Then, it was observed when the liquid molecular order is taken into account.[34] Finally, it was proven[35,36] under the hypothesis 13, and Monte Carlo simulations showed this mathematical property to be valid even for relatively short times.[37] On the basis of this theoretical development, the $\sqrt{\omega}$ dispersion of $j_2(\sigma = i\omega)$ was used to study the translational diffusion in viscous pure diamagnetic liquids[40] and then in solutions of stable paramagnetic free radicals.[41−43] In the present work, the long-time $t^{-3/2}$ of $g_2(t)$ will also serve to explore the electronic relaxation, in both the low- and medium-field ranges.

(P2) Within the Redfield perturbation approximation of a time-independent Zeeman Hamiltonian, the normalized longitudinal electronic TCF has essentially a monoexponential decay[44]

$$G_{||}^{nor}(t) = \exp(-t/T_{1e}(B_0)) \quad (15)$$

characterized by a single longitudinal electronic relaxation time $T_{1e}(B_0)$. This Redfield approximation is valid toward the high fields $B_0 \geq B_0^{Redfield}$, where the Redfield boundary field $B_0^{Redfield}$ is given by $B_0^{Redfield} \geq 0.1$ to 0.2 T for the majority of the Gd-(III) complexes. Moreover, when the static zero-field splitting (ZFS), which contributes to the electronic relaxation, tends to 0, we get $B_0^{Redfield} = 0$ and the Redfield approximation can be used for all field values.

(P3) Within the Redfield perturbation approximation of a time-independent Zeeman Hamiltonian, an approximate low-field expression of $G_\perp^{nor}(t)$ is simply

$$G_\perp^{nor}(t) \cong \exp(i\omega_s t)\exp(-t/\tau_{S0}) \quad (16)$$

where $\tau_{S0} \equiv T_{1e}(B_0 = 0)$ is the longitudinal electronic relaxation time at zero-field.

This can be proven as follows. Within this Redfield approximation, the transverse relaxation function $G_\perp^{nor}(t)$ is[18,45]

$$G_\perp^{nor}(t) = \exp(i\omega_s t)\sum_{i=1}^{4} w_i(B_0)\exp(-t/T_{2ie}(B_0)) \quad (17)$$

where the four weights $w_i(B_0)$ ($\sum_{i=1}^4 w_i(B_0) = 1$) and transverse electronic relaxation times $T_{2ie}(B_0)$ depend strongly on B_0. Now, at very small magnetic field, the transverse x and y directions of the laboratory frame become equivalent to its z direction taken to be along $\mathbf{B}_0$, so that $G_\perp^{nor}(t) = G_{||}^{nor}(t)$. According to that equality and eqs 15 and 17, we have

$$\sum_{i=1}^{4} w_i(B_0)\exp(-t/T_{2ie}(B_0)) \to G_\perp^{nor}(t)|_{B_0=0} = G_{||}^{nor}(t)|_{B_0=0} = \exp(-t/\tau_{S0}) \text{ as } B_0 \to 0 \quad (18)$$

In the low-field domain, substituting $\exp(-t/\tau_{S0})$ for the sum of the four exponentials in the Redfield expression 17, we have proven approximation 16 within the Redfield relaxation theory.

(40) Harmon, J. F. *Chem. Phys. Lett.* **1970**, *7*, 207−210.
(41) Fries, P. H.; Belorizky, E.; Minier, M.; Albrand, J. P.; Taïeb, M. C. *Mol. Phys.* **1982**, *47*, 1153−1158.
(42) Darges, G.; Müller-Warmuth, W. *J. Magn. Reson.* **1985**, *65*, 444−458.
(43) Belorizky, E.; Gillies, D. G.; Gorecki, W.; Lang, K.; Noack, F.; Rouc, C.; Struppe, J.; Sutcliffe, L. H.; Travers, J. P.; Wu, X. *J. Phys. Chem. A* **1998**, *102*, 3674−3680.
(44) Belorizky, E.; Fries, P. H. *Phys. Chem. Chem. Phys.* **2004**, *6*, 2341−2351.
(45) Hudson, A.; Lewis, J. W. E. *Trans. Faraday. Soc.* **1970**, *66*, 1297−1301.

Note that this approximation is often used as an ad hoc simplifying hypothesis for the Gd(III) complexes.[5,6]

2.2. Relaxivities. The OSPREs $R_{\alpha p}^{OS}$ are linear combinations[5,6,46] of the spectral densities $j_{2dir}(\omega)$ which according to their definitions (9) are integrals over the intermolecular dipolar TCF $g_2(t)$ given by eq 4. Very often, as[5,6] the ISPREs and 2SPREs, they are simply proportional to the number density N_S of the GdL complexes, which appears explicitely in the expression of $g_2(t)$. Then, the efficiency of a GdL complex, or more generally of a paramagnetic solute, to enhance R_1, R_2, or $R_{1\rho}$ can be defined as the corresponding PRE due to a 1 mM increase of the concentration of Gd(III) complex. This efficiency is named relaxivity. According to eq 2, the relaxivity r_α (α = 1, 2, 1ρ) is defined as[5,6]

$$r_\alpha \equiv \frac{R_{\alpha p}}{c_S[\mathrm{mM}]} = r_\alpha^{IS} + r_\alpha^{2S} + r_\alpha^{OS} \tag{19}$$

where $R_{\alpha p}$ is the PRE of type α, c_S [mM] is the concentration of complexes in mmol L^{-1}, and the IS, 2S, and OS relaxivities are $r_\alpha^{IS} \equiv R_{\alpha p}^{IS}/c_S$, $r_\alpha^{2S} \equiv R_{\alpha p}^{2S}/c_S$, and $r_\alpha^{OS} \equiv R_{\alpha p}^{OS}/c_S$, respectively. The number density N_S of the complexes, which appears in the expressions of $R_{\alpha p}^{IS}$, $R_{\alpha p}^{2S}$, $R_{\alpha p}^{OS}$, is readily derived from their concentration c_S [mM] as

$$N_S = 10^{-6} N_{\mathrm{Avogadro}} c_S\ [\mathrm{mM}] \tag{20}$$

It should be emphasized that the relaxivities defined by eq 19 are independent of the concentration c_S of the complexes only if the PREs increase linearly with it. This can be false for the OSPREs if the complex and the probe solute are charged species, especially at low ionic strengths,[47−50] or for all the PREs in the case of macromolecular complexes at concentrations above a few mM because of viscosity change.[12] In what follows, the PREs are assumed to be proportional to c_S so that the spectral densities involved in the expressions of the relaxivities are calculated for a concentration $c_S = 1$ mM, i.e., $N_S = 10^{-6} N_{\mathrm{Avogadro}}$.

2.3. Low-Frequency Expressions of the Longitudinal Outer-Sphere Paramagnetic Relaxation Enhancement.

2.3.1. Spectral Densities. We are now in a position to derive two low-frequency expressions of R_{1p}^{OS} or r_1^{OS}, which can be used to determine D and T_{1e} from suitable longitudinal nuclear relaxation measurements as a function of field. These expressions are based on the universal long-time behavior in $(Dt)^{-3/2}$ of the dipolar TCF $g_2(t)$ given by eq 14. Assume that the normalized TCF $G_{dir}^{nor}(t)$ (dir = ||,⊥) is of the form $G_{dir}^{nor}(t) = \exp(-i\omega_{Gdir}t)\exp(-t/T_e)$ where ω_{Gdir} is $\omega_{G||} \equiv 0$ and $\omega_{G\perp} \equiv \omega_S$. Also define ω_{dir} as $\omega_{||} \equiv \omega_I$ and $\omega_\perp \equiv 0$. The spectral densities $j_{2dir}(\omega_{dir})$ introduced by eq 9 can be expressed in terms of the transforms 5 and 6 giving $\tilde{g}_2(\sigma)$ and $j_2(\sigma)$ as

$$\begin{aligned} j_{2dir}(\omega_{dir}) &\equiv \frac{1}{\pi}\mathrm{Re}\int_0^\infty g_2(t)\exp(-i\omega t)\exp(-t/T_e)\,\mathrm{d}t \\ &= \frac{1}{\pi}\mathrm{Re}\tilde{g}_2(\sigma = i\omega + 1/T_e) \\ &= j_2(\sigma = i\omega + 1/T_e) \end{aligned} \tag{21}$$

where the Larmor angular frequency ω defined as $\omega \equiv \omega_{dir} + \omega_{Gdir}$ is $\omega = \omega_I$ for $j_{2||}$ and $\omega = \omega_S$ for $j_{2\perp}$. As shown in Appendix A (Supporting Information pp S1−S2), the spectral density $j_{2dir}(\omega_{dir})$ can be approximated as

$$j_{2dir}(\omega_{dir}) = j_2(0) - \frac{1}{9\pi}\frac{N_S}{D^{3/2}}\mathrm{Re}(\sqrt{i\omega + 1/T_e}) \tag{22}$$

with

$$j_2(0) \equiv \frac{1}{\pi}\int_0^\infty g_2(t)\,\mathrm{d}t \tag{23}$$

for sufficiently small ω and $1/T_e$ values. The validity range of the approximate formula 22 can be derived by estimating the duration Δt required for a notable variation of the long-time expression 14 of $g_2(t)$. The typical magnitude of $g_2(t)$ is given by its value $g_2(0)$ in the simple situation where the species M_I and GdL can be approximated as hard spheres, the spins I and S are located at the centers of these spheres, and the distribution of the complexes GdL with respect to M_I is uniform. Under these conditions, the interspin distance distribution function $g_{IS}^{site-site}$ simplifies to

$$g_{IS}^{site-site}(r) = \begin{cases} 1 \text{ if } r \geq b \\ 0 \text{ otherwise} \end{cases} \tag{24}$$

and, since $\rho(\mathbf{r}_0,\mathbf{r},t=0) = \delta(\mathbf{r} - \mathbf{r}_0)$, $g_2(0)$ becomes

$$g_2(0) = N_S \times \iiint_{r\geq b} \frac{Y_{2q}(\theta,\phi)}{r^3}\frac{Y_{2q}(\theta,\phi)^*}{r^3} r^2\,\mathrm{d}r\sin\theta\,\mathrm{d}\theta\,\mathrm{d}\phi = \frac{N_S}{3b^3} \tag{25}$$

According to eq 25, a notable variation of the long-time expression 14 of $g_2(t)$ with respect to $g_2(0)$ requires a duration Δt such as $(D\Delta t)^{3/2} > b^3$, i.e., $\Delta t > \tau$, where

$$\tau \equiv \frac{b^2}{D} \tag{26}$$

is the translational correlation time of the OS intermolecular motion. Thus, the limiting form of $\tilde{g}_2(\sigma)$ at small σ given in Appendix A corresponds to a small variation of $\exp(-\sigma t)$ over the duration τ, i.e., $\sigma\tau < 1$. The validity conditions of the approximation 22 are

$$\omega\tau < 1 \text{ and } \frac{\tau}{T_e} < 1 \tag{27}$$

2.3.2. Low Field. Assume that the static ZFS is small, so that the usual relaxation theory of Redfield for a dominant constant Zeeman Hamiltonian ("high-field" relaxation theory) can be applied. At low field, substituting the monoexponential decay $\exp(-t/\tau_{S0})$ for $G_{||}^{nor}(t)$ and the approximation 16 for $G_\perp^{nor}(t)$ in the definitions 9 of the spectral densities, these functions take the form 21

(46) Banci, L.; Bertini, I.; Luchinat, C. *Nuclear and Electron Relaxation*; VCH: Weinheim, 1991.
(47) Fries, P. H.; Patey, G. N. *J. Chem. Phys.* **1984**, *80*, 6253−6266.
(48) Fries, P. H.; Jagannathan, N. R.; Herring, F. G.; Patey, G. N. *J. Chem. Phys.* **1984**, *80*, 6267−6273.
(49) Fries, P. H.; Rendell, J.; Burnell, E. E.; Patey, G. N. *J. Chem. Phys.* **1985**, *83*, 307−311.
(50) Sacco, A.; Belorizky, E.; Jeannin, M.; Gorecki, W.; Fries, P. H. *J. Phys. II France* **1997**, *7*, 1299−1322.

$j_{2\|}(\omega_I) \cong j_2(\sigma = i\omega_I + 1/\tau_{S0})$ and

$$j_{2\perp}(0) \cong j_2(\sigma = i\omega_S + 1/\tau_{S0}) \quad (28)$$

Let λ_D be the OS relaxivity-variation parameter defined as

$$\lambda_D \equiv \frac{2}{45\pi}\gamma_I^2\gamma_S^2h^2S(S+1)10^{-6}N_{\text{Avogadro}} \quad (29)$$

Under the low-field validity conditions $\omega_S\tau < 1$ and $\tau/\tau_{S0} < 1$, the approximation 22 leads to the low-field expression of the longitudinal OS relaxivity

$$r_1^{\text{OS low-field}} = r_1^{\text{OS low-field}}(0,\infty) + \Delta r_1^{\text{OS low-field}} \quad (30)$$

with

$$r_1^{\text{OS low-field}}(0,\infty) = \frac{10}{3}Aj_2(0) \quad (31)$$

and

$$\Delta r_1^{\text{OS low-field}} = -\frac{\lambda_D}{D^{3/2}}\left[\text{Re}\sqrt{1/\tau_{S0}} + \frac{7}{3}\text{Re}\sqrt{i\frac{\gamma_S}{\gamma_I}2\pi\nu_I + 1/\tau_{S0}}\right] \quad (32)$$

In eqs 30 and 31, the argument $(0,\infty)$ stands for $B_0 = 0$ and $\tau_{S0} = \infty$. In eq 32 the dispersion at the electronic resonance frequency $\omega_S = (\gamma_S/\gamma_I)2\pi\nu_I$ stems from $j_{2\perp}(0)$. The dispersion at the nuclear resonance frequency $\omega_I = 2\pi\nu_I$ due to $j_{2\|}(\omega_I)$ is negligible at low field and is dropped in the expression of $\Delta r_1^{\text{OS low-field}}$.

2.3.3. Medium Field. Now, consider the medium field range such as $\omega_I\tau < 1$ and $\omega_S\tau \gg 1$. In water, for most of the Gd(III) complexes, this occurs for magnetic field values $B_0 \geq 0.5$ T. Then, the spectral density $j_{2\perp}(0)$ can be neglected because of the very rapid oscillations of $G_\perp^{\text{nor}}(t)$ and the general expression of r_1^{OS} reduces to

$$r_1^{\text{OS medium-field}} = Aj_{2\|}(\omega_I) \quad (33)$$

According to the property (P2), $G_\|^{\text{nor}}(t)$ is given by eq 15. Substituting this monoexponential decay for $G_\|^{\text{nor}}(t)$ in the definition 9 of the spectral density $j_{2\|}(\omega_I)$, the latter takes the form 21

$$j_{2\|}(\omega_I) \cong j_2(\sigma = i\omega_I + 1/T_{1e}(B_0)) \quad (34)$$

Under the medium-field validity conditions $\omega_I\tau < 1$ and $\tau/T_{1e}(B_0) < 1$, the approximation 22 leads to the medium-field expression of the longitudinal OS relaxivity at low nuclear resonance frequency $\omega_I = 2\pi\nu_I$

$$r_1^{\text{OS medium-field}} = r_1^{\text{OS medium-field}}(0,\infty) + \Delta r_1^{\text{OS medium-field}} \quad (35)$$

with

$$r_1^{\text{OS medium-field}}(0,\infty) = Aj_2(0) \quad (36)$$

and

$$\Delta r_1^{\text{OS medium-field}} = -\frac{\lambda_D}{D^{3/2}}\text{Re}\sqrt{i2\pi\nu_I + 1/T_{1e}(B_0)} \quad (37)$$

In eqs 35 and 36, the argument $(0,\infty)$ stands for $B_0 = 0$ and $T_{1e} = \infty$. According to eqs 31 and 36, we obtain the low-field/medium-field "10/3" relationship

$$r_1^{\text{OS low-field}}(0,\infty) = (10/3)r_1^{\text{OS medium-field}}(0,\infty) \quad (38)$$

which holds in real situations where the Redfield perturbation approximation of a time-independent Zeeman Hamiltonian is justified.

2.4. Transverse Relaxation and Longitudinal Relaxation in the Rotating Frame at Medium Field. In the medium field range such as $\omega_I\tau < 1$ and $\omega_S\tau \gg 1$, the transverse OS relaxivity r_2^{OS} is given by[5,6,46]

$$r_2^{\text{OS medium-field}} = A\left[\frac{2}{3}j_{2\|}(0) + \frac{1}{2}j_{2\|}(\omega_I)\right] \quad (39)$$

The longitudinal OS relaxivity $r_{1\rho}^{\text{OS}}$ in the rotating frame[38] has a similar expression[46]

$$r_{1\rho}^{\text{OS medium-field}} = A\left[\frac{2}{3}j_{2\|}(\omega_1) + \frac{1}{2}j_{2\|}(\omega_I)\right] \quad (40)$$

where $\omega_1 \equiv -\gamma_I B_1$ is the angular Larmor resonance frequency corresponding to the intensity B_1 of the radio frequency field.[38] For nonviscous solvents, the field dispersion due to B_1 is negligible, so that $j_{2\|}(\omega_1) \cong j_{2\|}(0)$ and $r_{1\rho}^{\text{OS medium-field}} \cong r_2^{\text{OS medium-field}}$. Under the medium-field validity conditions $\omega_I\tau < 1$ and $\tau/T_{1e}(B_0) < 1$, it can be shown as above that the low-frequency expressions of the OS relaxivities 39 and 40 are

$$r_2^{\text{OS medium-field}} \cong r_{1\rho}^{\text{OS medium-field}} = r_2^{\text{OS medium-field}}(0,\infty) + \Delta r_2^{\text{OS medium-field}} \quad (41)$$

with

$$r_2^{\text{OS medium-field}}(0,\infty) = r_{1\rho}^{\text{OS medium-field}}(0,\infty) = \frac{7}{6}Aj_2(0) = \frac{7}{6}r_1^{\text{OS medium-field}}(0,\infty) \quad (42)$$

and

$$\Delta r_2^{\text{OS medium-field}} = -\frac{\lambda_D}{D^{3/2}}\left[\frac{2}{3}\text{Re}\sqrt{1/T_{1e}(B_0)} + \frac{1}{2}\text{Re}\sqrt{i2\pi\nu_I + 1/T_{1e}(B_0)}\right] \quad (43)$$

In eqs 41 and 42, the argument $(0,\infty)$ stands for $B_0 = 0$ and $T_{1e} = \infty$.

Finally, introduce the useful mixed OS relaxivity $r_{\text{mix}}^{\text{OS medium-field}}$ as the linear combinations

$$r_{\text{mix}}^{\text{OS medium-field}} \equiv \frac{3}{2}\left(r_2^{\text{OS medium-field}} - \frac{1}{2}r_1^{\text{OS medium-field}}\right) \cong \frac{3}{2}\left(r_{1\rho}^{\text{OS medium-field}} - \frac{1}{2}r_1^{\text{OS medium-field}}\right) \quad (44)$$

of the transverse OS relaxivity (or longitudinal OS relaxivity in the rotating frame) and of the longitudinal OS relaxivity. According to eqs 33 and 39, $r_{\text{mix}}^{\text{OS medium-field}}$ is given by

$$r_{\text{mix}}^{\text{OS medium-field}} = Aj_{2\|}(0) \quad (45)$$

which can be rewritten as

$$r_{\mathrm{mix}}^{\mathrm{OS\ medium-field}} = r_{\mathrm{mix}}^{\mathrm{OS\ medium-field}}(\infty) + \Delta r_{\mathrm{mix}}^{\mathrm{OS\ medium-field}} \quad (46)$$

with

$$r_{\mathrm{mix}}^{\mathrm{OS\ medium-field}}(\infty) = Aj_2(0) = r_1^{\mathrm{OS\ medium-field}}(0,\infty) \quad (47)$$

and

$$\Delta r_{\mathrm{mix}}^{\mathrm{OS\ medium-field}} = -\frac{\lambda_D}{D^{3/2}}\mathrm{Re}\sqrt{1/T_{1e}(B_0)} \quad (48)$$

Again, in eqs 46 and 47, the arguments 0 and ∞ of $r_{\mathrm{mix}}^{\mathrm{OS\ medium-field}}(\infty)$ and $r_1^{\mathrm{OS\ medium-field}}(0,\infty)$ stand for $B_0 = 0$ and $T_{1e} = \infty$, respectively. Clearly, at medium field, the longitudinal electronic relaxation rate $1/T_{1e}(B_0)$ can be obtained from the experimental knowledge of $r_1^{\mathrm{OS\ medium-field}}$, $r_2^{\mathrm{OS\ medium-field}}$ (or $r_{1\rho}^{\mathrm{OS\ medium-field}}$), and D.

As mentioned at the beginning of section 2, the universal square-root terms of the OSPREs are the major sources of PRE dispersion at low frequency. Indeed, for the probe solutes, which do not coordinate the metal, the possible 2SPREs display small low-frequency variations in ω_S^2 and ω_I^2 at low and medium field, respectively.[10] Note that similar small variations occur[5,6] for the ISPREs of probe solutes such as water, which directly bind to the metal, provided that the complex rotates sufficiently rapidly as the usual contrast agents do in water and standard nonviscous solvents. Under these conditions, the IS- and 2SPREs can be considered as frequency independent with respect to the OSPREs. Finally, it should be emphasized that the zero-field OS relaxivity values $r_1^{\mathrm{OS\ low-field}}(0,\infty)$, $r_1^{\mathrm{OS\ medium-field}}(0,\infty)$, $r_2^{\mathrm{OS\ medium-field}}(0,\infty)$, $r_{1\rho}^{\mathrm{OS\ medium-field}}(0,\infty)$, and $r_{\mathrm{mix}}^{\mathrm{OS\ medium-field}}(\infty)$ given by eqs 31, 36, 42, and 47 are simply proportional to the dipolar TCF integral $\int_0^\infty g_2(t)\,\mathrm{d}t$ according to the definition 23 of the spectral density $j_2(0)$. They are independent of the electronic relaxation and just give information on the relative spatial dynamics of the species carrying the interacting spins.

3. Experimental Section

Our goal is to study the proton relaxation rates of water HOD, methanol CH_3OD, and *tert*-butyl alcohol $(CH_3)_3COD$ in heavy water solutions over a large frequency range between 10 kHz and 500 MHz. The longitudinal relaxtion rates were measured at low field by using a low-resolution FFC relaxometer[28] which cannot separare the signals of the protons in different chemical environments. In the CH_3OD or $(CH_3)_3COD$ solutions, the HOD concentration should be kept as small as possible, so that the residual HOD signal remains a few percent of that of the investigated CH_3 protons. Therefore, extra-pure D_2O and highly D-enriched alcohols are needed for the preparation of the CH_3OD or $(CH_3)_3COD$ solutions.

Materials. The Gd and Lu complexes were prepared from $LnCl_3 \cdot 6H_2O$ salts (Aldrich 99.9%) according to the published procedures.[27] The complex purity and formulas were checked by elemental analysis performed by the Service Central d'Analyses (Vernaison, 69, France). The solutions of Ln(tpatcn) complexes were prepared by dissolving the isolated complexes in deuterium oxide. Extra-pure deuterium oxide (99.96% atom D, euriso-top) was required for the stock solution of Gd(tpatcn) complexes (6.5 ± 0.1 mmol L^{-1}), but standard deuterium oxide (99.9% atom D, euriso-top) could be used for the solution of [Lu(tpatcn)] complexes (5.0 ± 0.1 mmol L^{-1}). Methanol CH_3OD (methyl alcohol-*d*, 99.5+ atom % D) and *tert*-butyl alcohol $(CH_3)_3COD$ (2-methyl-2-propan(ol-d), 99 atom % D) were purchased from Aldrich.

Self-Diffusion Coefficient Measurements. The self-diffusion coefficients D_X of Lu(tpatcn), HOD, CH_3OD, and $(CH_3)_3COD$ were obtained by measuring the attenuation of the spin−echo which arises from diffusive dephasing under the influence of pulsed field gradients.[26] Let $S(0)$ and $S(g)$ be the amplitudes of the echo without field gradient and with pulsed field gradients of amplitude g, respectively. Denote the pulse duration by δ and the diffusion time interval between the starts of the gradient pulse trains by Δ. The pulsed gradient spin−echo (PGSE) sequences employed were (i) the standard Stejskal−Tanner sequence such as

$$\frac{S(g)}{S(0)} = \exp[-\gamma_I^2 g^2 \delta^2 D_X(\Delta - \delta/3)] \quad (49)$$

and (ii) the simple stimulated-echo experiment with bipolar gradients proposed by Jerschow and Müller (JM) (see Figure 1b of ref 51) such as

$$\frac{S(g)}{S(0)} = \exp[-\gamma_I^2 g^2 \delta^2 D_X(\Delta - \delta/3 - \tau_{\mathrm{JM}}/4)] \quad (50)$$

τ_{JM} being an additional delay between the radio frequency and gradient pulses. These sequences were applied to the proton signals of the molecules on a Varian U400 operating at 400 MHz. In both cases, the durations δ, Δ, and τ_{JM} were fixed, and the attenuation of the echo was recorded as a function of the square g^2 of the gradient amplitude. A simple fitting of the exponential decay of the echo attenuation $S(g)/S(0)$ vs g^2 by more than an order of magnitude gave the self-diffusion coefficients D_X of the molecules with an accuracy of about 5%.

Nuclear Magnetic Relaxation Dispersion Measurements. The proton relaxation times T_1, T_2, and $T_{1\rho}$ of the probe solutes were measured at 400 MHz on a Varian Unity 400 spectrometer and at 500 MHz on a Bruker Advance 500 and a Varian Unity+ 500. The temperature of the samples was set to 298 K with the help of the temperature calibration samples provided by the manufacturers. The T_1 and T_2 values were measured using the standard inversion−recovery and Carr−Purcell, Meiboom−Gill sequences,[38] respectively. The relaxation time $T_{1\rho}$ was obtained[38] by rotating the equilibrium magnetization in the direction of the radio frequency field B_1 by a $\pi/2$ pulse and, then, by recording the time evolution of this magnetization locked along the B_1 direction.

Longitudinal relaxation times T_1 were measured from 10 kHz to 28 MHz with a commercial Spinmaster FFC 2000 Stelar relaxometer[28,29] (Stelar srl, Mede PV, Italy) of the new generation. The prepolarized (PP) and nonpolarized (NP) sequences (see Figure 1 of ref 29) were used below and above ≅12 MHz, respectively. A high polarization field B_{pol} corresponding to a proton resonance frequency of 28 MHz was employed in the PP experiments. Thus, the NMRD profiles of the rather dilute protons (2 to 3 mol L^{-1}) of the probe solutes were recorded easily with a satisfactory signal/noise ratio.

The relaxation measurements were generally repeated at least two times. At 500 MHz, when passing from the Bruker Advance 500 to the Varian Unity+ 500, the measured T_1 values may vary by 1%, and the T_2 or $T_{1\rho}$ values, by 2%, when these relaxation times are in the range 50 to 150 ms as in the present study. These uncertainties define limits to the experimental accuracy which may be difficult to improve.

4. Results

It is well-known that electronic relaxation is one important factor affecting the relaxivity of Gd(III) complexes.[5,6] Recently, the Gd(tpatcn) and $[Gd(dotam)H_2O]^{3+}$ complexes sketeched in

(51) Jerschow, A.; Müller, N. *J. Magn. Reson.* **1997**, *125*, 372−375.

Chart 1

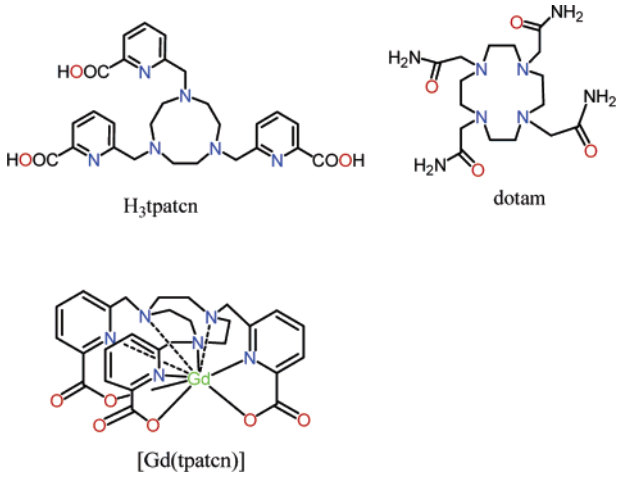

Chart 1, with dotam = (1,4,7,10-tetrakis-(carbamoylmethyl)-1,4,7,10-tetrazacyclododecane), were shown to display remarkably sharp EPR lines,[52] i.e., slow transverse electronic spin relaxation, especially at X-band. In the Gd(tpatcn) complex, the Gd(III) ion is fully encapsulated in the tpatcn ligand and no water molecule is coordinated to this ion, so that the PREs of the nuclear spins of the water hydrogen atoms, and more generally of solutes which do not bind to tpatcn, are of pure outer-sphere origin.

The D_2O solutions of the probe solutes water HOD, methanol CH_3OD, and *tert*-butyl alcohol $(CH_3)_3COD$ contained the following concentrations of interacting species: In the HOD solution, we had $c_S = 5.0 \pm 0.1$ mM and [HOD] = 2.1 M. In the CH_3OD solution, we had $c_S = 5.04 \pm 0.1$ mM and [CH_3OD] = 1.0 M. In the $(CH_3)_3COD$ solution, we had $c_S = 5.09 \pm 0.1$ mM and [$(CH_3)_3COD$] = 0.37 M. For each probe solute, the experimental relaxivities r_α (α = 1, 2, 1ρ, mix) were obtained from equations 1, 19, and 44 under the hypothesis that the corresponding relaxation rates $R_{\alpha 0}$ in the absence of Gd(tpatcn) complexes are equal and display negligible field dispersion. At 298 K and 400 MHz the values of the longitudinal relaxation rate R_{10} were found to be about 0.05, 0.08, and 0.4 s^{-1} for the probe solutes HOD, CH_3OD, and $(CH_3)_3COD$, respectively. In these solutions, we checked that the dissolved paramagnetic oxygen has negligible contributions to the relaxation rates with respect to those of Gd(tpatcn), which are largely dominant.

4.1. Low-Field Study. The longitudinal relaxivities r_1 of the protons of HOD, CH_3OD, and $(CH_3)_3COD$ due to Gd(tpatcn) were measured in heavy water at 298 K as a function of the proton resonance frequency ν_I in the range 10 kHz to 28 MHz. The relaxivity profiles are reported in Figure 1 vs $\sqrt{\nu_I[\mathrm{MHz}]}$, ν_I being expressed in MHz.

4.1.1. Relaxivity Magnitudes. The HOD relaxivity r_1[HOD] decreases from 6 to 2.2 s^{-1} mM^{-1}, when ν_I grows from 10 kHz to 28 MHz. These values are significantly smaller than those of the Gd(dtpa) or Gd(dota) CA which has a similar size but one inner-sphere coordinated water molecule.[16] Thus, the magnitude of r_1[HOD] can be explained by a pure OS mechanism. At a given field, the magnitudes of r_1 are in the order r_1[HOD] < r_1[CH_3OD] < r_1[$(CH_3)_3COD$]. This can be qualitatively explained as follows. We have $r_1 = R_{1p}^{OS}/c_S$ [mM] and the spectral densities $j_{2\mathrm{dir}}(\omega_{\mathrm{dir}})$ involved in the expression 8 of R_{1p}^{OS} can be written as[31,33,34]

$$j_{2\mathrm{dir}}(\omega_{\mathrm{dir}}) \equiv \frac{N_S}{\pi D b} \vec{j}_{2\mathrm{dir}}(\omega_{\mathrm{dir}}\tau) \qquad (51)$$

where the auxiliary functions $\vec{j}_{2\mathrm{dir}}(\omega_{\mathrm{dir}}\tau)$ are reduced spectral densities. On one hand, in this low-field domain, $\vec{j}_{2\mathrm{dir}}(\omega_{\mathrm{dir}}\tau)$ depends moderately on the size of the probe solute M_I = HOD, CH_3OD, or *t*-$(CH_3)_3COD$ interacting with the Gd(III) complex. Furthermore, the collision diameters b of Gd(tpatcn) with these species have similar values. On the other hand, the relative diffusion coefficient D of Gd(tpatcn) with respect to M_I is the sum

$$D = D_I + D_S \qquad (52)$$

of the self-diffusion coefficients D_I and D_S of M_I and Gd(tpatcn) reported in Table 1.

The value of D is mainly D_I, since the self-diffusion coefficient D_S of the large Gd(tpatcn) complex is significantly smaller than D_I. Therefore, the reduced spectral densities $\vec{j}_{2dir}(\omega_{\mathrm{dir}}\tau)$ given by eq 51, and consequently r_1, are roughly inversely proportional to D_I. This explains why r_1 notably increases as the self-diffusion of the probe solute interacting with Gd(tpatcn) becomes slower and slower.

4.1.2. Frequency Dispersion. For all profiles, r_1 decreases by a factor of about 3, when ν_I grows from 10 kHz to 28 MHz (HOD and $(CH_3)_3COD$) or 20 MHz (CH_3OD). This factor is near to 10/3. According to the expression 8 of R_{1p}^{OS}, such a factor of decrease is expected as soon as the following two conditions (i) and (ii) are met when the field value increases in the low-field domain, i.e., changes from 0 to ≅0.5 T in the present study: (i) the spectral density $j_{2||}(\omega_I)$ displays only a

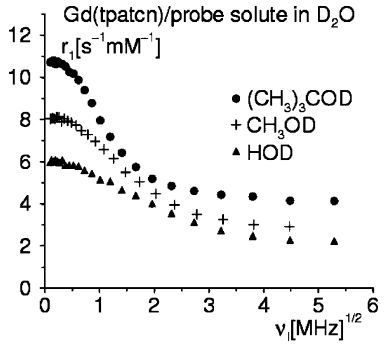

Figure 1. Measured longitudinal relaxivities r_1 vs the square-root of the resonance frequency ν_I of the HOD, CH_3OD, and $(CH_3)_3COD$ protons due to Gd(tpatcn) in heavy water D_2O at 298 K. The values were obtained between 10 kHz and 28 MHz using a FFC Stelar relaxometer of the new generation.

Table 1. Measured Self-Diffusion Coefficients by the PGSE Technique in Heavy Water D_2O at 298 K[a]

species M_I	HOD	CH_3OD	$(CH_3)_3COD$
D_I (10^{-5} cm^2 s^{-1})	1.8	1.1	0.57
$D = D_I + D_S$ (10^{-5} cm^2 s^{-1})	2.18	1.48	0.95

[a] The self-diffusion coefficient D_S of Gd(tpatcn) is assumed to be equal to the measured value 0.38 × 10^{-5} cm^2 s^{-1} of the very similar complex Lu(tpatcn). The values $D = D_I + D_S$ of the relative diffusion coefficients are also reported.

(52) Borel, A.; Kang, H.; Gateau, C.; Mazzanti, M.; Clarkson, R. B.; Belford, R. L. *J. Phys. Chem.*, submitted.

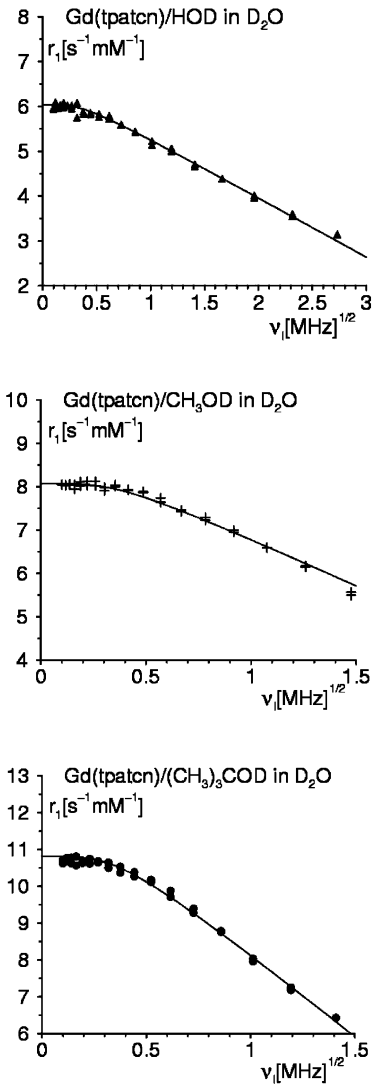

Figure 2. Low-field longitudinal relaxivities r_1 vs the square-root of the resonance frequency ν_I of the HOD, CH_3OD, and $(CH_3)_3COD$ protons due to Gd(tpatcn) in heavy water D_2O at 298 K. The continuous curves are the theoretical relaxivities $r_1^{\text{OS low-field}}$ given by eqs 30 and 32 with the fitted parameters of Table 2.

slight variation because of the modest influence of a rather slow electronic relaxation, and (ii) the spectral density $j_{2\perp}(0)$ markedly drops from $j_{2\perp}(0) = j_{2\parallel}(0)$ to approximately 0 because of a notable dispersion at the electronic resonance frequency ω_S due to the oscillations of $\bar{G}_\perp(t)$. The two properties (i) and (ii), referred to as the "10/3" validity conditions, are necessary in order to have a low-field range, where the expression of $r_1^{\text{OS low-field}}$ given by eqs 30 to 32 applies. Practically, they correspond to the low-field/high-field "10/3" relationship 38. Since the "10/3" validity conditions hold, it is informative to zoom on the low-field ranges, where the various profiles show linear decays in $\sqrt{\nu_I}$. This zooming can be seen in Figure 2.

The relaxivities r_1 are of the form $r_1 = \text{constant} - m\sqrt{\nu_I}$, approximately in the interval 0.5 to 5 MHz for HOD, and in the interval 0.25 to 2.5 MHz for CH_3OD and $(CH_3)_3COD$. Now, the low-field expression $r_1^{\text{OS low-field}}$ of the longitudinal OS relaxivity, which is given by eqs 30 and 32 and has to be adjusted, clearly reproduces the experimental square-root behavior for B_0 such as $1/\tau_{S0} \ll \gamma_S/\gamma_I\ 2\pi\nu_I$. The quantities $r_1^{\text{OS low-field}}(0,\infty)$, D, and $1/\tau_{S0}$ involved in $r_1^{\text{OS low-field}}$ can be considered as parameters, which are fitted so as to reproduce the measured longitudinal relaxivity. The fitted values are reported in Table 2.

They lead to theoretical values of $r_1^{\text{OS low-field}}$, represented in Figure 2 by continuous curves, which display the right low-field dispersion behavior.

4.1.3. Accuracy. To estimate the accuracy of the values of the molecular parameters obtained from relaxivity profile analysis, it is useful to compare them with their counterparts derived from different experimental methods.

The relative diffusion coefficients D of Table 2 are in excellent agreement with the values of Table 1 obtained by the independent PGSE methods[26,51] presented in section 3. It should be noted that the low-frequency square-root behavior of the OS relaxivity is sensitive to translational diffusion over a duration of the order of a few correlation times τ corresponding to Brownian displacements over a few collision diameters b. Relaxivity profile analysis probes translational diffusion at the nanometer scale. The situation is quite different in the case of the measurement of self-diffusion coefficients by PGSE methods. The self-diffusion coefficients of M_I and LuL, representing GdL, are measured independently through the random translational displacements $\sqrt{6D_X\Delta}$ ($X = I,S$) of these molecules, which for typical PGSE experiments with a field gradient pulse separation $\Delta = 100$ ms are of the order of 10 μm. It is remarkable that two independent methods exploring the Brownian motion on one hand at a molecular scale (nm) and on the other hand at a semimacroscopic scale (μm) lead to the same values of translational diffusion coefficients.

As discussed in section 2.3.1, the influence of the rapidity D of the relative diffusion on the spectral density $j_{2\perp}(0)$, i.e., on R_{1p}^{OS} or r_1^{OS}, is related to the variation of $\exp(-i\omega_S t)$ over the duration τ and increases with $\omega_S\tau$, i.e., with the sizes of the species M_I and GdL, and also with $1/D$ according to the definition 26 of τ. Practically, the dispersion of r_1^{OS} vs ω_S is a measurable effect that yields an estimate of D when the condition $\omega_S\tau > \epsilon_D$ is met with $\epsilon_D \cong 0.02$.

The values of the electronic relaxation rate $1/\tau_{S0}$ at zero-field reported in Table 2 are in overall good agreement with previous determinations. They bracket the value $1/\tau_{S0}^{\text{adhoc}} = 4.8 \times 10^8\ \text{s}^{-1}$, which was inferred by Gateau et al.[27] from the NMRD profile analysis of the protons of light water H_2O and is the limiting zero-field value of the ad hoc formula of the longitudinal electronic relaxation rate[16,53]

$$\frac{1}{T_{1e}^{\text{ad hoc}}} = \frac{12}{5}(\Delta^{\text{ad hoc}})^2\tau_v^{\text{ad hoc}}\left[\frac{1}{1+\omega_S{}^2(\tau_v^{\text{ad hoc}})^2} + \frac{4}{1+4\omega_S{}^2(\tau_v^{\text{ad hoc}})^2}\right] \quad (53)$$

such as

$$\frac{1}{\tau_{S0}^{\text{ad hoc}}} \equiv \frac{1}{T_{1e}^{\text{ad hoc}}(B_0=0)} = 12(\Delta^{\text{ad hoc}})^2\tau_v^{\text{ad hoc}} = 4.8 \times 10^8\ \text{s}^{-1} \text{ and } \tau_v^{\text{ad hoc}}(298\ \text{K}) = 0.4\ \text{ps} \quad (54)$$

The estimates $7 \times 10^8\ \text{s}^{-1}$ and $7.5 \times 10^8\ \text{s}^{-1}$ fitted from the CH_3OD and $(CH_3)_3COD$ relaxivity profiles are very near the value $1/\tau_{S0}^{\text{EPR}} = 6.14 \times 10^8\ \text{s}^{-1}$, which is derived from the

Table 2. Adjusted Relative Diffusion Coefficients D, Zero-Field Electronic Relaxation Rates $1/\tau_{S0}$, and Zero-Field OS Relaxivity Values $r_1^{\text{OS low-field}}(0,\infty)$ in the Case of an Ideal Infinitely Slow Electronic Relaxation to Yield the Low-Field Relaxivity Profiles of HOD, CH_3OD, and $(CH_3)_3COD$ Due to Gd(tpatcn) in Heavy Water D_2O at 298 K[a]

species M_I	HOD	CH_3OD	$(CH_3)_3COD$
$r_1^{\text{OS low-field}}(0,\infty)(s^{-1}\,mM^{-1})$	6.92	10.13	15.38
D (10^{-5} $cm^2\,s^{-1}$)	2.21	1.45	0.87
$1/\tau_{S0}$ ($10^8\,s^{-1}$)	4.5	7.	7.5
τ (10^{-10} s)	1.0	1.7	3.4

[a] The quantity c_S is the concentration of Gd(tpatcn) expressed in mmol L^{-1}. Rough estimates of the translational correlation time τ are also reported.

molecular parameters obtained by Borel et al.[52] through a variable temperature and EPR frequency study of Gd(tpatcn) in light water. More precisely, $1/\tau_{S0}^{\text{EPR}}$ is taken to be the zero-field value of the longitudinal electronic relaxation rate $1/T_{1e}(B_0)$ given by the Redfield-limit analytical expression[15,44]

$$\frac{1}{T_{1e}(B_0)} = \frac{2}{5}a_2^2\tau_R\left[\frac{1}{1+\omega_S^2\tau_2^2}+\frac{4}{1+4\omega_S^2\tau_2^2}\right] + \frac{12}{5}a_{2T}^2\tau'\left[\frac{1}{1+\omega_S^2\tau'^2}+\frac{4}{1+4\omega_S^2\tau'^2}\right] \quad (55)$$

with

$$\tau_2 \equiv \tau_R/6 \text{ and } \frac{1}{\tau'} \equiv \frac{1}{\tau_2}+\frac{1}{\tau_v} \quad (56)$$

In eqs 55 and 56 the molecular parameters used to calculate $1/\tau_{S0}^{\text{EPR}} = 1/T_{1e}(B_0 = 0)$ are chosen as follows. The static and transient Gd(III) ZFS parameters $a_2 = 0.0661 \times 10^{10}$ rad s^{-1} and $a_{2T} = 0.2322 \times 10^{10}$ rad s^{-1}, together with the characteristic time $\tau_v = 1.19$ ps at 298 K of the vibration−distortion of the complex, are the values fitted by Borel et al.[52] under the hypothesis that Gd(tpatcn) has the reasonable rotational correlation time value $\tau_R(H_2O) \equiv 1/D_R(H_2O) = 500$ ps in light water at 298 K. These parameter values yield theoretical EPR properties reproducing their experimental counterparts, measured at several temperatures and frequencies in light water.[52] Now, the present experiments were carried out in D_2O. The rotational correlation time τ_R is proportional to the solvent viscosity η according to the Stokes−Einstein formula,[12,18] so that its value in D_2O at 298 K is taken to be $\tau_R(D_2O) = [\eta(D_2O)/\eta(H_2O)]\tau_R(H_2O) = 615$ ps, since[54] $\eta(D_2O)/\eta(H_2O) = 1.23$.

It should be noted that the $1/\tau_{S0}$ values derived from relaxivity profiles have relative errors of at least 5 to 10%. These errors mainly stem from the difficulty of the experimental determination of the zero-field difference

$$|\Delta r_1^{\text{OS low-field}}(0)| = r_1^{\text{OS low-field}}(0,\infty) - r_1^{\text{OS low-field}}(0) = \frac{10}{3}\frac{\lambda_D}{D^{3/2}}\text{Re}\sqrt{1/\tau_{S0}} \quad (57)$$

which is all the more accurate because the percentage variation $|\Delta r_1^{\text{OS low-field}}(0)|/r_1^{\text{OS low-field}}(0,\infty)$ of $r_1^{\text{OS low-field}}(0,\infty)$ at $B_0 = 0$ is large. This percentage variation caused by the finite value of $1/\tau_{S0}$ is 15, 21, and 30% for the HOD, CH_3OD, and $(CH_3)_3COD$ relaxivity profiles, respectively. Two complementary reasons can be invoked to explain this increase with the probe solute size. First, this percentage variation is proportional to $1/\sqrt{D}$ because $|\Delta r_1^{\text{OS low-field}}(0)| \propto 1/D^{3/2}$ according to eq 57 and $r_1^{\text{OS low-field}}(0,\infty) \propto j_2(0) \propto 1/D$ according to eqs 22, 31, and 51. Second, as discussed in section 2.3.1, the influence of the electronic relaxation on the spectral densities j_{2dir}, i.e., on r_1^{OS}, is related to the variation of $\exp(-t/\tau_{S0})$ over the duration τ and increases with τ/τ_{S0}, i.e., with the size of the species M_I and again with $1/D$ according to the definition 26 of τ. Practically, the value of the electronic relaxation rate $1/\tau_{S0}$ can be derived from its effects on r_1^{OS} when the condition $\tau/\tau_{S0} > \epsilon_e$ is met with $\epsilon_e \cong 0.02$. To sum it up, the accuracy of the $1/\tau_{S0}$ determination through relaxivity profile analysis increases as the probe M_I has a larger and larger size and a slower and slower self-diffusion. As a counterexample, the HOD molecule with its small size and rapid self-diffusion only provides a rough estimate of $1/\tau_{S0}$. For instance, the fitted value 4.5×10^8 s^{-1} given in Table 2 could be 20% larger without notable alteration of the quality of the fit.

The low-field validity conditions $\omega_S\tau < 1$ and $\tau/\tau_{S0} < 1$ of section 2.3.2 allow one to use the low-field expressions 30 and 32. However, according to the previous discussions, the relative diffusion coefficient D and the electronic relaxation rate $1/\tau_{S0}$ can be measured from their effects on the relaxivity profile only if $1/D$ and $1/\tau_{S0}$ are large enough. The conditions of the successful application of the low-field low-frequency relaxivity profile analysis to the determination of D and $1/\tau_{S0}$ are

$$\epsilon_D < \omega_S\tau < 1 \text{ and } \epsilon_e < \tau/\tau_{S0} < 1 \quad (58)$$

with $\epsilon_D \cong 0.02$ and $\epsilon_e \cong 0.02$. It should be noted that the definition 26 of τ rests on that of the collision diameter b which is only an approximate quantity for nonspherical species. Therefore, the bounds of the conditions 58 are also approximate values which can easily vary by 50%.

4.1.4. Collision Geometry. The general theory of the OSPRE for species M_I and GdL, which are coupled by an anisotropic intermolecular potential and/or dissolved in a polar solvent like water, is complicated.[55] Indeed, the dipolar TCF $g_2(t)$ defined by eq 4 depends on the interspin functions $g_{IS}^{\text{site-site}}(r_0)$ and $\rho(\mathbf{r}_0,\mathbf{r},t)$, which stem from the molecular pair distribution function (PDF) and the molecular propagator describing the time evolution of the relative position and orientation of the interacting species. Two treacherous routes can be envisaged to obtain $g_2(t)$. First, the molecular PDF can be calculated with the help of the sophisticated molecular integral equation theory of the statistical physics of liquids[56] and the molecular propagator obtained by Brownian translational and rotational random walks,[55] the diffusion coefficients of which can be determined by independent PGSE measurements.[26,51] Second, molecular dynamics (MD) can serve to generate trajectories of the interspin position $\mathbf{r}$, the average over which directly gives the expression 3 defining $g_2(t)$, without resorting to the intermediate functions $g_{IS}^{\text{site-site}}(r_0)$ and $\rho(\mathbf{r}_0,\mathbf{r},t)$. Unfortunately, obtaining reasonable diffusion coefficients by MD simulations is still a difficult

(53) Powell, D. H.; Merbach, A. E.; González, G.; Brücher, E.; Micskei, K.; Ottaviani, M. F.; Köhler, K.; von Zelewsky, A.; Grinberg, O. Y.; Lebedev, Y. S. *Helv. Chim. Acta* **1993**, *76*, 2129−2146.
(54) Marcus, Y. *Ion solvation*; John Wiley: New York, 1985; pp 87, 93−94.
(55) Fries, P. H.; Belorizky, E.; Bourdin, N.; Cinget, F.; Gagnaire, D.; Gorecki, W.; Jeannin, M.; Vottéro, Ph. *THEOCHEM* **1995**, *330*, 335−345.
(56) Fries, P. H.; Richardi, J.; Rast, S.; Belorizky, E. *Pure Appl. Chem.* **2001**, *73*, 1689−1703.

challenge posed by the design of accurate intermolecular potentials.[57] Thus, the simulated OSPREs, which are strongly affected by the rapidity of diffusion, are expected to be poorly reliable. Moreover, simulations involving dilute species are computer demanding. To sum it up, precise information on the collision dynamics of the species M_I and GdL beyond their relative diffusion coefficient is not easily accessible from the OSPREs because the latter arise from intricate positional and orientational correlations evolving with time.

Because of the difficulties of a detailed description of the collision of the species involved in the OSPREs, the usual approach is to content oneself with the ABHF model proposed independently by Ayant and Belorizky[31] (AB) and Hwang and Freed[32] (HF). In this model, the spins I and S are assumed to be located at the centers of the interacting species approximated as hard spheres diffusing in a viscous continuum. The spectral density $j_2(\sigma)$ of the dipolar TCF $g_2(t)$ is a rational function of $\sqrt{\sigma\tau}$

$$j_2(\sigma) = \frac{N_S}{\pi D b}\mathrm{Re}\frac{4+x}{3(9+9x+4x^2+x^3)} \text{ with } x \equiv \sqrt{\sigma\tau} \quad (59)$$

At $\sigma = 0$, it reduces to

$$j_2(0) = \frac{N_S}{\pi D b}\frac{4}{27} \quad (60)$$

so that the expression 31 of the zero-field OS relaxivity in the case of an ideal infinitely slow electronic relaxation becomes

$$r_1^{\text{OS low}-\text{field}}(0,\infty) = \frac{40}{81}A\frac{10^{-6}N_{\text{Avogadro}}}{\pi D b} \quad (61)$$

By equating this expression to the fitted values of $r_1^{\text{OS low}-\text{field}}(0,\infty)$ reported in Table 2, estimates of the collision diameter b are 3.8, 4.0, and 4.3 Å for HOD, CH_3OD, and $(CH_3)_3COD$, respectively. These values have reasonable magnitudes and show the expected increase with the size of the probe solute M_I. However, they are somewhat too short because the ABHF model neglects the close packing and anisotropic shapes of the molecules, the eccentricity of the proton spin I, and a possible attractive potential of M_I by Gd(tpatcn) due to H-bonding and/or hydrophobic forces. Each of these molecular features results in an increase of the reduced dipolar spectral density $\tilde{j}_2(0)$ which is typically[34] of the order of 20% because of the packing of spherical molecules and a few percent because of the spin eccentricity. Should $\tilde{j}_2(0)$ be 25% larger than the estimate 4/27 of the ABHF model, then the collision diameters b would be 4.7, 5.0, and 5.4 Å for HOD, CH_3OD, and $(CH_3)_3COD$, respectively. These values are near those obtained from the crystallographic data of Gd(tpatcn) and compact molecular models of the probe solutes M_I. They can be used to roughly calculate the translational correlation time τ defined by eq 26. For each probe solute, the estimate of τ obtained from the relative diffusion coefficient of Table 2 is also reported in this table. It increases by a factor of 3.4 when passing from the small HOD molecule to the larger $(CH_3)_3COD$ solute. This rather large dynamical range clearly supports the universal character of the long time decay of the dipolar TCF $g_2(t)$ given by eq 14.

(57) Mahoney, M. W.; Jorgensen, W. L. *J. Chem. Phys.* **2001**, *114*, 363−366.

In the usual picture[5,6] of the OSPRE of the water protons due to Gd(III) complexes, the outer-sphere motion is given by the ABHF model of a force-free translational diffusion applied to the interspin vector $\mathbf{r}$ with a collision distance a_{GdH} taken to be the minimal distance of approach of Gd(III) with a proton of a noncoordinated water molecule. For contrast agents such as $[Gd(DTPA)]^{2-}$, a_{GdH} is typically[12,16] 3.5 to 3.6 Å. Although this range of values is compatible with simple molecular models and provides a reasonable OSPRE contribution to the relaxivity, it should be kept in mind that it rests on the ABHF model, which is only valid for centered spins and neglects molecular packing and possible H-bonding.

4.2. Medium-Field Study. The linear variation in $\mathrm{Re}\sqrt{i2\pi\nu_I + 1/T_{1e}(B_0)}$ of the medium-field expression $r_1^{\text{OSmedium}-\text{field}}$ given by eqs 35 and 37 occurs in the proton frequency interval $\nu_{I\,\text{min}}^{\text{medium}-\text{field}} < \nu_I < \nu_{I\,\text{max}}^{\text{medium}-\text{field}}$. According to section 2.3.3, the lower bound $\nu_{I\,\text{min}}^{\text{medium}-\text{field}}$ depends on the value of the translational correlation time τ. For the studied M_I/Gd(tpatcn) pairs, it lies between 50 and 100 MHz. The upper bound $\nu_{I\,\text{max}}^{\text{medium}-\text{field}}$ is that of the low-field $\sqrt{\nu_I}$ validity range times $\gamma_S/\gamma_I = 658$. According to the low-field relaxivity profiles of Figure 2, $\nu_{I\,\text{max}}^{\text{medium}-\text{field}}$ should be about 1500 MHz for HOD, 1000 MHz for CH_3OD, and 600 MHz for $(CH_3)_3COD$. Contrary to the low-field relaxation profiles, which can be measured on a single relaxometer, the medium-field investigation generally needs a range of spectrometers operating at different field values B_0. Below 90 MHz, an electromagnet can be used to produce a variable magnetic field with a resolution often between 1 and 10 ppm. In the interval 100 to 200 MHz, there are NMR imagers operating at about 128 MHz (3 Ts), and rather old high-resolution spectrometers with cryomagnets working at 200 MHz can be found. At 300 MHz and above up to 900 MHz, commercial spectrometers with cryomagnets, for both liquid and solid state NMR, are available, but again they operate only at a fixed given magnetic field. Thus, above 90 MHz, the NMR profile can be recorded only at a small number of discrete frequencies. Furthermore, the temperature of the sample in the various instruments should be kept the same by a correct calibration so that the variation of R_{1p}^{OS} is entirely due to the change of magnetic field B_0.

Assume that the longitudinal electronic relaxation rate $1/T_{1e}(B_0)$ of Gd(tpatcn) is given by eqs 55 and 56. It is a decreasing function of magnetic field B_0. The static and transient ZFS contributions, which are proportional to $a_2^2\tau_R$ and $a_{2T}^2\tau'$, rapidly decay as $1/B_0^2$ for $\omega_S\tau_2 \geq 2$ and $\omega_S\tau' \geq 2$, respectively. The static contribution, which is largely dominant at zero field, becomes less than 1% of the small transient term for $B_0 > 1$ T, since the rotational correlation time $\tau_2 = 83$ ps is much longer than $\tau' \cong \tau_2 = 1.19$ ps. Therefore, the predicted values of $1/T_{1e}(B_0)$ are smaller than 7×10^6 s^{-1} for $B_0 > 1$ T. Now, a staightforward generalization of the discussion of subsection 4.1.3 shows that the conditions of successful determination of accurate D and $1/T_{1e}(B_0)$ values from a medium-field relaxivity profile are

$$\epsilon_D < \omega_S\tau < 1 \text{ and } \epsilon_e < \tau/T_{1e}(B_0) < 1 \quad (62)$$

with $\epsilon_D \cong 0.02$ and $\epsilon_e \cong 0.02$. For the three probe solutes, according to the estimates of τ reported in Table 2, we expect $\tau/T_{1e}(B_0) \leq \epsilon_e$ if $B_0 > 1$ T, so that deriving accurate values of

Table 3. Experimental Relaxivities r_1, r_2, $r_{1\rho}$, and r_{mix} of the HOD, CH_3OD, and $(CH_3)_3COD$ Protons Due to the Gd(tpatcn) Complexes in D_2O at 298 K for the Two Proton Resonance Frequencies 400 and 500 MHz[a]

species	HOD		CH_3OD		$(CH_3)_3COD$	
r_1 (s^{-1} mM^{-1})	400 MHz	500 MHz	400 MHz	500 MHz	400 MHz	500 MHz
experiment	1.682	1.616	2.215	2.104	2.78	2.496
theory (static and transient ZFS)	1.63	1.578	2.20	2.10	2.81	2.60
r_2 (s^{-1} mM^{-1})	400 MHz	500 MHz	400 MHz	500 MHz	400 MHz	500 MHz
experiment	2.29	2.24	3.09	3.07	4.40	4.34
$r_{1\rho}$ (s^{-1} mM^{-1})	400 MHz	500 MHz	400 MHz	500 MHz	400 MHz	500 MHz
experiment	2.23	2.24	3.11	3.07	4.48	4.31
r_{mix} (s^{-1} mM^{-1})	400 MHz	500 MHz	400 MHz	500 MHz	400 MHz	500 MHz
experiment	2.12	2.14	2.98	3.03	4.58	4.61
theory (static and transient ZFS)	2.04	2.05	2.98	2.99	4.48	4.50
theory ($T_{1e}^{ad\ hoc}$)	1.89	1.92	2.70	2.74	3.88	3.97

[a] For each probe solute, the experimental value of r_{mix} is taken to be the average of the r_2 and $r_{1\rho}$ determinations. The independent measured values of r_1 and r_{mix} are compared with the theoretical predictions obtained by using as parameters the relative diffusion constants D and the zero-field OS relaxivity value $r_1^{OS\ low-field}(0,\infty)$ derived at low field. The electronic relaxation is described by a model of fluctuating static and transient ZFS or an ad hoc approach.

$1/T_{1e}(B_0)$ from the medium-field relaxivity profiles should not be possible. However, the medium-field study will allow us to show the self-consistency of the method and discriminate between the electronic relaxation models underlying the expressions 53, 54 of $1/T_{1e}^{ad\ hoc}$ and 55, 56 of $1/T_{1e}$. For that purpose, the measurements were performed at the proton resonance frequencies $\nu_I = 400$ and 500 MHz of the spectrometers available to our laboratory.

The measured relaxivities r_1, r_2, and $r_{1\rho}$ of HOD, CH_3OD, and $(CH_3)_3COD$ are reported in Table 3 together with the mixed relaxivity $r_{mix} \equiv {}^3/_2(r_2 - r_1/2)$.

The values of r_2 and $r_{1\rho}$, which in principle should be identical, can differ by about 2%. This gives an estimate of the best attainable accuracy for these properties. Given the scattter of the r_1 values to within 1%, the experimental precision on r_{mix} is in the range 2 to 3%. For the three probes, r_1 shows a measurable drop when ν_I increases from 400 to 500 MHz, whereas r_{mix} does not change. To assess the self-consistency of the method, the medium-field theoretical relaxivity $r_1^{OS\ medium-field}$ was calculated from eqs 35, 37, and 38 by using as parameters the relative diffusion coefficient D and the OS relaxivity value $r_1^{OS\ low-field}(0,\infty)$ determined at low field and reported in Table 2. The theoretical mixed relaxivity $r_{mix}^{OS\ medium-field}$ was obtained similarly from eqs 46 to 48. The theoretical values $r_1^{OS\ medium-field}$ and $r_{mix}^{OS\ medium-field}$ of r_1 and r_{mix}, which account for the time fluctuations of both the static and transient ZFS Hamiltonians and are calculated by using the electronic relaxation rate $1/T_{1e}$ given by eqs 55 and 56, are presented in Table 3 with the label "static and transient ZFS". They are in excellent agreement with their experimental counterparts for the three probe solutes. This demonstrates that the parameters of the relaxivities determined at low field are suitable to get accurate relaxivity values at medium field, which establishes the self-consistency of the method. This also supports the fluctuating static and transient ZFS model predicting rates $1/T_{1e}$, which are smaller than 7×10^6 s^{-1}, thus leading to theoretical values of r_{mix} that are only about 2% smaller than their maxima corresponding to an infinitely slow longitudinal electronic relaxation. On the contrary, the values 2.1×10^8 and 1.6×10^8 s^{-1} of $1/T_{1e}^{ad\ hoc}$ at 400 and 500 MHz given by eqs 53, 54 are much too large. Indeed, they lead to theoretical relaxivities r_{mix} given in Table 3 with the label "$T_{1e}^{ad\ hoc}$", which are significantly smaller than the experimental data.

5. Practical Implementation

Several ways of extracting dynamical information from the limiting behavior of the relaxivities r_1 and r_{mix} are possible. Here, a few simple routes to exploiting the potentialities of the method are summarized in a self-contained way. The key parameter governing the validity of the OS relaxivity limiting behavior is the translational correlation time τ defined by eq 26 where b is the collision diameter of the metal complex ML with the probe solute M_I and D their relative diffusion coefficient. An estimate of b can be obtained from CPK models or molecular modeling softwares. The relative diffusion coefficient D defined by eq 52 is the sum of the self-diffusion coefficients D_I of M_I and D_S of ML, which can be estimated from the Stokes−Einstein law,[28] possibly corrected by microviscosity factors.[34,58,59] The self-diffusion coefficients D_I and $D'_S \cong D_S$ of a diamagnetic analogue M′L of ML can also be measured by the PGSE technique.[26,51]

General Requirements for the Probe Solutes. The possible candidates M_I are species which do not coordinate the metal, do not have charge−charge Coulomb interaction with the metal complex, and carry observable nuclear spins I that are mainly relaxed by the intermolecular dipolar magnetic interactions with the metal electronic spins S. The latter condition is fulfilled by nuclear spins $I = {}^1/_2$ or nuclear spins $I > {}^1/_2$ of small quadrupole moments as soon as the concentration of metal complexes is larger than a few mM. Among the possible molecules the choice rests on the field range and on a rough estimate of the longitudinal electronic relaxation rate $1/T_{1e}(B_0)$, as explained hereafter.

Let $\omega_I = 2\pi\nu_I$ and $\omega_S = 2\pi\nu_S$ be the Larmor angular frequencies of the nuclear and electronic spins, respectively.

Low-Field Domain. $\omega_S\tau < 1$. Only the longitudinal relaxivity r_1 is concerned. Let τ_{S0} be the electronic relaxation time at zero-field. The following additional two conditions should be met

$$\tau/\tau_{S0} < 1 \text{ and } 0.02 < \omega_S\tau \qquad (63)$$

The first inequality $\tau/\tau_{S0} < 1$ expresses that τ_{S0} is significantly longer than τ and ensures that the limiting OS behavior of r_1 is not quenched by a too fast electronic relaxation. The condition $0.02 < \omega_S\tau$ leads to a relaxivity dispersion with field, which is large enough to provide information about D and τ_{S0}. Under

(58) Spernol, A.; Wirtz, K. *Z. Naturforsch., a* **1953**, *8*, 522−532.
(59) Gierer, A..; Wirtz, K. *Z. Naturforsch., a* **1953**, *8*, 532−538.

the conditions 63, the relaxivity r_1 is expressed by eqs 30 and 32. Following the discussion at the end of section 2, the method can be easily extended to account for a 2S relaxation mechanism. Then, the purely OS relaxivity value $r_1^{\text{OS low-field}}(0,\infty)$ has to be replaced by a more general term $r_1^{\text{low-field}}(0,\infty)$, which represents the sum of the values of the OS and 2S relaxivities at zero field in the ideal case of an infinitely long electronic relaxation time $\tau_{S0} \gg \tau$. The conditions 63 can be verified by simply checking that the r_1 profile has an overall linear decrease vs $\sqrt{\nu_I}$ with a possible attenuation at zero field due to the finite τ/τ_{S0} value, as shown in Figure 2. The values of $r_1^{\text{low-field}}(0,\infty)$, D, and $1/\tau_{S0}$ are fitted so that the theoretical profile reproduces the experiment. Note that the probe solutes M_I should be sufficiently soluble to get a good signal/noise ratio of the observed nuclear spins. This requires a proton concentration above $\cong$2 mol L^{-1} on the Stelar instrument[28] with the presently commercial probe. The range of applicability of the method would be extended by an improvement of the Stelar probe sensitivity or by using a dual-magnet high-resolution relaxometer of the type designed by Bryant et al.[60]

Medium-Field Domain. $\omega_I\tau < 1 \ll \omega_S\tau$. Both the longitudinal relaxivity r_1 and the mixed relaxivity r_{mix} are concerned. Let $T_{1e}(B_0)$ be the electronic relaxation time in the relaxation field B_0.

The longitudinal relaxivity r_1 can be used if the following additional two conditions are met

$$\tau/T_{1e}(B_0) < 1 \text{ and } 0.02 < \omega_I\tau \tag{64}$$

The first inequality $\tau/T_{1e}(B_0) < 1$ expresses that $T_{1e}(B_0)$ is significantly longer than τ and ensures that the limiting OS behavior of r_1 is not quenched by a too fast electronic relaxation. The condition $0.02 < \omega_I\tau$ leads to a relaxivity dispersion with field, which is large enough to provide information about D and $T_{1e}(B_0)$. Under the conditions 64, the relaxivity r_1 is expressed by eqs 35 and 37. To account for a 2S relaxation mechanism the purely OS relaxivity value $r_1^{\text{OS medium-field}}(0,\infty)$ has to be replaced by a more general term $r_1^{\text{medium-field}}(0,\infty)$ incorporating this additional effect. Again, the values of $r_1^{\text{medium-field}}(0,\infty)$, D, and $1/T_{1e}(B_0)$ can be derived from a fit of the theoretical profile to its experimental counterpart. Note that $r_1^{\text{low-field}}(0,\infty) = (10/3)r_1^{\text{medium-field}}(0,\infty)$.

The mixed relaxivity r_{mix} can be used if the sole additional condition is fulfilled

$$\tau/T_{1e}(B_0) < 1 \tag{65}$$

Again, this inequality ensures that the limiting OS behavior of r_{mix} is not quenched by a too fast electronic relaxation. Then, the limiting behavior of r_{mix} is given by eqs 46 and 48. The purely OS relaxivity value $r_{\text{mix}}^{\text{OS medium-field}}(\infty)$ can be replaced by a more general term $r_{\text{mix}}^{\text{medium-field}}(\infty)$ accounting for a 2S relaxation effect. Information about $r_{\text{mix}}^{\text{medium-field}}(\infty)$, D, and $T_{1e}(B_0)$ can be derived from a fit of the theoretical profile to its experimental counterpart.

As discussed in section 4, the relative diffusion coefficient D can be obtained as the sum of the measured self-diffusion coefficients of M_I and of a diamagnetic analogue of ML by the independent PGSE technique. Then, only the electronic relaxation rates and the ideal zero-field values $r_1^{\text{low-field}}(0,\infty)$ or $r_1^{\text{medium-field}}(0,\infty)$ have to be fitted from the relaxivity profiles. Furthermore, if $r_1^{\text{medium-field}}(0,\infty)$ is determined by a longitudinal relaxivity study, the electronic relaxation rate $1/T_{1e}(B_0)$ is readily calculated from the r_{mix} profile using eqs 46 and 48, since $r_{\text{mix}}^{\text{medium-field}}(\infty) = r_1^{\text{medium-field}}(0,\infty)$ according to eq 47.

Suggested Probe Solutes. In view of the previous discussion, they can be classified as follows. Working with low-resolution instruments implies that the probes bear only one kind of equivalent nuclei. Working at low field on a conventional spectrometer or a Stelar relaxometer requires a probe concentration typically $\geq$0.2 M and an observed nuclei of high gyromagnetic ratios such as ^{1}H, ^{19}F, or ^{31}P. Neutral, globular, soluble probes are generally recommended. In heavy water, they can be nonpolar like *p*-dioxane or have an electric dipole like methanol CH_3OD and *tert*-butyl alcohol $(CH_3)_3COD$, provided that the charge-dipole attraction with the metal complex is not too high. In perdeuterated organic solvents, especially of low dielectric constants, where the electrostatic attractions are less screened by the solvent,[56,61] nonpolar probes such as neopentane $(CH_3)_4C$ and tetramethylsilane $(CH_3)_4Si$ are preferable. For neutral metal complexes in heavy water, tetramethylammonium $(CH_3)_4N^+$ and tetramethylphosphonium $(CH_3)_4N^+$ cations can be envisaged. Fluorinated anions such as hexafluorophosphate PF_6^- and triflate $CF_3SO_3^-$ can be appropriate in light water, but the absence of hyperfine scalar interaction should be checked.[56] On conventional high-resolution spectrometers or a dual-magnet high-resolution relaxometer of the type designed by Bryant et al.,[60] the restriction that the probes bear only one kind of equivalent nuclei can be removed and more bulky solutes can be used. For instance, the tetraalkylammonium ions of varying sizes and self-diffuion coefficients can be suitable probes for neutral metal complexes in heavy water.

6. Conclusion

Using three probe solutes covering a range of self-diffusion speeds, we have shown how the outer-sphere (OS) paramagnetic relaxation enhancements (PREs) of $1/T_1$, $1/T_2$, and $1/T_{1\rho}$ due to the Gd(tpatcn) complex can serve to simultaneously determine the relative diffusion coefficient D of the complex with respect to the probe solute and the longitudinal electronic relaxation rate $1/T_{1e}$ of Gd(III). The method rests on the long-time behavior of the time correlation function (TCF) $g_2(t)$ of the dipolar magnetic coupling between an observed nuclear spin on the probe solute and the Gd(III) electronic spin. Indeed, when the probe solute does not have a charge−charge Coulomb interaction with the Gd(III) complex, $g_2(t)$ has a universal decay in $(Dt)^{-3/2}$, independent of the geometries of the interacting species and of their local ordering in the solution. Starting from this long-time behavior we derived simple low-frequency analytical expressions of the PREs in terms of D, $\int_0^\infty g_2(t)\,dt$, and $1/T_{1e}$, which allow one to determine these quantities by fitting the analytical expressions to their experimental counterparts. At zero magnetic field, the fitted electronic relaxation time $\cong$ 1500 ps of the Gd(tpatcn) complex is the longer value reported to date for a gadolinium complex (650 ps for the $Gd(dota)^-$ contrast agent[5]) in agreement with a previous estimate inferred from the

(60) Wagner, S.; Dinesen, T. R. J.; Rayner, T.; Bryant, R. G. *J. Magn. Reson.* **1999**, *140*, 172−178.

(61) Stell, G.; Patey, G. N.; Høye, J. S. *Adv. Chem. Phys.* **1981**, *48*, 183−328.

relaxivity profile in light water. Taking advantage of the particularly slow electronic relaxation of the Gd(tpatcn) complex, we demonstrated the self-consistency of the method by cross-checking the low- and medium-field results. The accuracy on the determination of D, $\int_0^\infty g_2(t)\,dt$, and $1/T_{1e}$ was estimated to be about 5, 5, and 10 to 20%, respectively.

The method can be extended to other situations. First, the longitudinal PRE studies at low field can be used to measure the relative diffusion coefficients involving paramagnetic molecules and ions of slow low-field electronic relaxation. This includes the stable nitroxide radicals and the Gd(III) or Mn(II) complexes, like the Gd(tpatcn) and the Mn(II) aqua ion, which have a slow longitudinal electronic relaxation because of suitable coordination structures. Second, at low field, paramagnetic metal cations of electronic spins $S \geq 1$ often have electronic relaxation times[46] $T_{1e} = \tau_{S0} \leq 10^{-10}$ s, which are shorter than the translational correlation time τ, so that the method does not apply. However, it was recently shown[44,62] that $1/T_{1e}$ is still given by an expression of the form 55 and 56 if $B_0 > 3$ to 5 T, even in the case of static and transient ZFS as large as 1 cm^{-1}. For these field values, T_{1e} rapidly increases as B_0^2 and becomes significantly longer than τ in the range $B_0 \geq B_{0\,min}^{medium-field}$, where the method is again valid. To our knowledge, this is the only model-independent way to measure longitudinal electronic relaxation times above 3 to 5 T. Third, the method can be extended to metal complexes giving rise to inner- and/or second-sphere PREs. One difference concerns the frequency-independent terms $r_1^{OS\ low-field}(0,\infty)$ and $r_1^{OS\ medium-field}(0,\infty)$, which occur in the relaxivity analytical expressions to be fitted and correspond to the outer-sphere relaxivity values for an ideal infinitely slow electronic relaxation. These terms have to be replaced by more general quantities which incorporate additional similar contributions stemming from the inner- and second-sphere relaxation mechanisms. Quite generally, they provide one with an information about the intermolecular dynamics of the interacting partners, which is not blurred by the electronic relaxation. This can be useful to better understand the effects of the intermolecular forces on the outer-sphere PRE and/or assess the presence of a second-sphere PRE. Fourth, the relative diffusion is explored at the nanometer scale over a few collision diameters of the interacting species, which can thus be confined in very small restricted volumes without preventing the validity of the method. Applications to porous media and vesicles can be envisaged. The above-mentioned potentialities should be investigated, and studies along these lines are underway.

(62) Fries, P. H.; Belorizky, E. *J. Chem. Phys.* **2005**, *123*, 124510-1−124510-15.

Acknowledgment. P.H.F. is grateful to P. A. Bayle, B. Gennaro, and A. Galkin for helping to use the Varian Unity 400 and Bruker Advance 500, the Varian Unity+ 500, and the FFC 2000 Stelar relaxometer, respectively. He thanks Prof. D. Canet for illuminating discussions on relaxation measurements. The interest of Dr. M. Defranceschi in the relaxometric exploration of the microdynamics of lanthanide complexes in solution and the financial support of the Nuclear Energy Division of the CEA for the purchase of the relaxometer are highly appreciated. This research was carried out in the frame of the EC COST Action D-18 "Lanthanide Chemistry for Diagnosis and Therapy" and the European Molecular Imaging Laboratories (EMIL) network. This work is dedicated to Prof. Elie Belorizky, in honor of his 40-year distinguished work in many areas of magnetism.

Supporting Information Available: In pp S1−S2, we propose a mathematical proof of the analytical limiting behavior of the Laplace transform $\tilde{g}_2(\sigma)$ of the intermolecular dipolar time correlation function as $\sigma \rightarrow 0$. The low-frequency approximation 22 of the spectral densities stems from this fundamental property and is the basis of all the analytical expressions of the relaxation rates derived in this work. This material is available free of charge via the Internet at http://pubs.acs.org.

JA052800L